

HIGH PERFORMANCE MACRO SYNTHETIC FIBER REINFORCED  
CONCRETE

A THESIS SUBMITTED TO  
THE GRADUATE SCHOOL OF NATURAL AND APPLIED SCIENCES  
OF  
MIDDLE EAST TECHNICAL UNIVERSITY

BY

ÇAĞRI ÖZTÜRK

IN PARTIAL FULFILLMENT OF THE REQUIREMENTS  
FOR  
THE DEGREE OF MASTER OF SCIENCE  
IN  
CIVIL ENGINEERING

MARCH 2018



Approval of the thesis:

**HIGH PERFORMANCE MACRO SYNTHETIC FIBER REINFORCED  
CONCRETE**

submitted by **ÇAĞRI ÖZTÜRK** in partial fulfillment of the requirements for the degree of **Master of Science in Civil Engineering Department, Middle East Technical University** by,

Prof. Dr. Halil Kalıpçılar  
Director, Graduate School of **Natural and Applied Sciences**

\_\_\_\_\_

Prof. Dr. İsmail Özgür Yaman  
Head of Department, **Civil Engineering**

\_\_\_\_\_

Prof. Dr. İsmail Özgür Yaman  
Supervisor, **Civil Engineering, METU**

\_\_\_\_\_

**Examining Committee Members:**

Prof. Dr. Mustafa Tokyay  
Civil Engineering, METU

\_\_\_\_\_

Prof. Dr. İsmail Özgür Yaman  
Civil Engineering, METU

\_\_\_\_\_

Assoc. Prof. Dr. Sinan Turhan Erdoğan  
Civil Engineering, METU

\_\_\_\_\_

Assoc. Prof. Dr. Serdar Göktepe  
Civil Engineering, METU

\_\_\_\_\_

Prof. Dr. Mustafa Şahmaran  
Civil Engineering, Hacettepe University

\_\_\_\_\_

**Date:**

\_\_\_\_\_

**I hereby declare that all information in this document has been obtained and presented in accordance with academic rules and ethical conduct. I also declare that, as required by these rules and conduct, I have fully cited and referenced all material and results that are not original to this work.**

Name, Last Name: Çađrı ÖZTÜRK

Signature :

## **ABSTRACT**

### **HIGH PERFORMANCE MACRO SYNTHETIC FIBER REINFORCED CONCRETE**

Öztürk, Çağrı

M.S., Department of Civil Engineering

Supervisor : Prof. Dr. İsmail Özgür Yaman

March 2018, 78 pages

Since concrete is a brittle construction material, it has the tendency to fail in a brittle manner after the occurrence of the first crack when it is subjected to a certain amount of load. Therefore, this property of concrete makes almost impossible for it to be used in load carrying structural elements without reinforcement. This reinforcement is usually utilized by a structural steel reinforcement such as rebar and wire mesh. The structural steel reinforcements compensate the low resistance against the tensile strength of the plain concrete by taking over the tensile stresses under different loading conditions. Nowadays, in addition to steel reinforcement randomly dispersed small sized fibers can also be utilized to improve the mechanical properties such as toughness of concrete.

The aim of this study is to determine the toughness of high performance macrosynthetic fibers. In order to obtain high performance, fiber dosages up to 2.7% was utilized with a highly viscous matrix. The toughness parameters were investigated by two different panel test methods which are; i) ASTM C1550: Standard Test Method for Flexural Toughness of Fiber Reinforced Concrete, and ii) EFNARC Square Panel Test Method.

As a result of the thesis study, it was found out that, with increasing fiber dosage, the energy absorption capacity of concrete improved significantly. Moreover, based on the energy absorption capacities obtained from the round and square specimens, an equation with good reliability was derived to describe the relation between the two test methods.

Keywords: Macro Synthetic Fibers, Test Methods, Energy Absorption Capacity, High Performance Fiber Reinforced Concrete

## ÖZ

### YÜKSEK PERFORMANSLI MAKRO SENTETİK FİBER KATKILI BETON

Öztürk, Çağrı

Yüksek Lisans, İnşaat Mühendisliği Bölümü

Tez Yöneticisi : Prof. Dr. İsmail Özgür Yaman

Mart 2018, 78 sayfa

Beton gevrek bir yapı malzemesi olduğu için belirli bir miktarda yüke maruz kaldığında ilk çatlaktan sonra gevrek bir tarzda kırılma eğilimi gösterir. Böylelikle, bu özellik betonu yük taşıyıcı yapısal elemanlarda donatısız kullanmayı neredeyse imkansız hale getirir. Bu donatılar bar ve çelik hasır gibi yapısal çelik donatılardır. Yapısal çelik donatılar farklı yükleme şartlarında, çekme dayanımını üstlenerek, donatısız betonun düşük çekme dayanımını özelliğini kapatırlar. Günümüzde, çelik donatılara ilaveten, rastgele dağılmış küçük boyutlu fiber donatılar, tokluk gibi betonun mekanik özelliklerini birçok yönden iyileştirmek amacıyla betonarme yapılarda kullanılmaktadır.

Bu tez çalışmasında, yüksek performanslı makro sentetik fiber katkıli betonların tokluklarını ölçmektir. Yüksek performans elde etmek için ise, %2.7 oranında fiber dozajı yüksek akışkan bir matriksle kullanılmıştır. Bu tez çalışmasında, makro sentetik fiber donatılı betonlar kullanılarak betonun tokluk parametreleri i) ASTM C 1550 ve ii) EFNARC test metotları kullanarak incelenmiştir.

Bu tez çalışmasının sonunda, artan fiber dozajı ile betonun enerji absorbe kapasitesinin

belirgin bir şekilde, arttığı görülmüştür. Dahası, kare ve yuvarlak numunelerin test sonuçlarından, iki farklı test metodu arasında enerji bazında iyi bir ilişki elde edilmiştir.

Anahtar Kelimeler: Makro Sentetik Fiber, Test Metotları, Enerji Yutma Kapasitesi, Yüksek Performanslı Fiber Katkılı Beton

*To My Family Members; İzgü, Şeref, Hatice, and Burcu ÖZTÜRK*

## ACKNOWLEDGMENTS

I would like to express my deep appreciation to my thesis supervisor Prof. Dr. İsmail Özgür Yaman for his patient guidance, enthusiastic encouragement and valuable advices during the development and preparation of this thesis. His willingness to give his time and to share his experiences has brightened my path. Mr. Yaman will be always my mentor in both professional and educational area.

I would like also to give heartfelt thanks to Dr. Burhan Alam for his contribution in every part of this work, starting from the laboratory stage to the end of this thesis preparation stage. No matter the time it was, he always answered my questions by supporting and enhancing my knowledge with his broad perspective in this field. I will be always thankful to Mr. Alam through my whole life.

Another valuable person I would like to thank, is my classmate Oğuz Hetemoğlu. He was always with me, especially during the laboratory work, and he shared all his knowledge and effort with me.

My special thanks to my father; Eng. Şeref ÖZTÜRK who encouraged me to apply to the master program and always drew a road map for me in every stage of my life. I will always take my father as a model in my life. I am always with you dad.

I would like also to thank another wonderful person of my life: my wife İzgü ÖZTÜRK, the expectant mother of my upcoming child. During the thesis study, unintentionally I neglected her. I want to apologize to her for the weekends which were full of my thesis. She always waited me patiently and appreciated what I did in this life. I am sure, you will continue being my greatest support and I will be the fiber reinforced protective layer of our family.

Last but not least, my thanks to the first ladies of my life; my mother Hatice ÖZTÜRK

and my sister Dr. Dt. Burcu ÖZTÜRK. You are the strongest support for me. If I submit my thesis study today, this is because of your continuous support. I am so glad to have you.

## TABLE OF CONTENTS

ABSTRACT . . . . .	v
ÖZ . . . . .	vii
ACKNOWLEDGMENTS . . . . .	x
TABLE OF CONTENTS . . . . .	xii
LIST OF TABLES . . . . .	xvi
LIST OF FIGURES . . . . .	xviii
LIST OF ABBREVIATIONS . . . . .	xxii
CHAPTERS	
1 INTRODUCTION . . . . .	1
1.1 General . . . . .	1
1.2 Scope and Objective . . . . .	2
2 LITERATURE REVIEW . . . . .	3
2.1 Historical Use of Fibers . . . . .	3
2.2 Definition of Toughness . . . . .	3
2.2.1 Load-Deflection Response of Fiber Reinforced Concrete . . . . .	6
2.3 Fiber Types . . . . .	7
2.3.1 Synthetic Fibers . . . . .	9

	2.3.1.1	Polypropylene Fibers Used in This Study	10
	2.3.1.2	Modified Olefin . . . . .	12
	2.3.2	Steel Fibers . . . . .	12
2.4		Mechanical Characteristics of Fiber Reinforced Concrete . .	14
	2.4.1	Compressive Strength . . . . .	15
	2.4.2	Flexural Strength . . . . .	16
	2.4.3	Modulus of Elasticity . . . . .	17
	2.4.4	Splitting Tensile Strength . . . . .	17
	2.4.5	Impact Resistance . . . . .	18
2.5		Fiber Properties Affecting Mechanical Characteristics of FRC Concrete . . . . .	20
	2.5.1	Fiber Aspect Ratio . . . . .	20
	2.5.2	Concrete Matrix and Elastic Modulus of Fibers . .	22
	2.5.3	The Effect of Fiber Orientation, Geometry, Dispersion and Shape . . . . .	23
2.6		Test Methods For Determining Flexural Toughness of Fiber Reinforced Concrete . . . . .	24
	2.6.1	Centrally Loaded Round Panel Method . . . . .	25
	2.6.1.1	Centrally Loaded Square Panel Method	27
	2.6.1.2	Comparison and Correlation of Round and Square Plate Test Results . . . . .	29
3		EXPERIMENTAL STUDY . . . . .	31
	3.1	Experimental Plan . . . . .	31
	3.2	Mixture Proportions . . . . .	32
	3.2.1	Cementitious Materials . . . . .	32

3.2.2	Fiber . . . . .	34
3.2.3	Superplasticizer . . . . .	35
3.2.4	Aggregates . . . . .	36
3.2.5	Water . . . . .	36
3.3	Test Equipment . . . . .	37
3.3.1	The Molds . . . . .	37
3.3.2	Mixer . . . . .	38
3.3.3	Loading Frame . . . . .	38
3.4	Experimental Procedure . . . . .	40
3.4.1	The Mixing and Casting Process . . . . .	40
3.4.2	The Testing Process . . . . .	41
3.5	Data Evaluation Method . . . . .	42
3.6	Measuring the Center Point Deflection . . . . .	42
4	TEST RESULTS . . . . .	45
4.1	Fresh Concrete Test Results . . . . .	45
4.2	Square Panel Test Data . . . . .	46
4.2.1	NPFC Square Samples . . . . .	46
4.2.2	HPFC Square Samples . . . . .	51
4.2.3	Comparison of NPFC and HPFC Square Samples . . . . .	55
4.3	Round Panel Test Data . . . . .	58
4.3.1	NPFC Round Samples . . . . .	58
4.3.2	HPFC Round Samples . . . . .	63
4.3.3	Comparison of NPFC and HPFC Round Samples . . . . .	67

4.4	Round vs Square Plate Energy Relationship . . . . .	69
5	CONCLUSION AND RECOMMENDATION . . . . .	71
5.1	Conclusion . . . . .	71
5.2	Recommendation . . . . .	73
	REFERENCES . . . . .	75

## LIST OF TABLES

### TABLES

Table 2.1	Typical properties of synthetic fibres (Bentur and Mindess 2007) . . .	9
Table 2.2	Properties of various types of polypropylene fibers (Singh, 2011) . . .	11
Table 2.3	The performance of steel fiber reinforced concrete compared to unreinforced concrete (Bothma 2013) . . . . .	14
Table 2.4	Modulus of rupture of changing fiber volume fraction (Bothma 2013).	16
Table 2.5	Impact strength test results (Anbuvelan 2014). . . . .	19
Table 3.1	Number of specimens . . . . .	32
Table 3.2	Mix designs . . . . .	33
Table 3.3	Major oxide composition of cement . . . . .	33
Table 3.4	The mechanical and physical properties of fibers (EPC 2016) . . . . .	34
Table 3.5	Properties of superplasticizer “Glenium51” from BASF (BASF 2013)	35
Table 3.6	Aggregate test results . . . . .	37
Table 4.1	Fresh concrete samples test results . . . . .	45
Table 4.2	Thickness of NPFC 3 square . . . . .	47
Table 4.3	Thickness of NPFC 6 Square . . . . .	48
Table 4.4	Thickness of NPFC 9 Square . . . . .	49

Table 4.5	Thickness of HPFC 12 square . . . . .	51
Table 4.6	Thickness of HPFC 18 square . . . . .	52
Table 4.7	Thickness of HPFC 24 square . . . . .	53
Table 4.8	Thickness of NPFC 3 round . . . . .	59
Table 4.9	Thickness of NPFC 6 round . . . . .	60
Table 4.10	Thickness of NPFC 9 round . . . . .	61
Table 4.11	Thickness of HPFC 12 round . . . . .	63
Table 4.12	Thickness of HPFC 18 round . . . . .	64
Table 4.13	Thickness of HPFC 24 round . . . . .	65
Table 4.14	Maximum energy in different volume fractions for round and square panels . . . . .	69

## LIST OF FIGURES

### FIGURES

Figure 2.1	Effect of fiber type in toughness (FHA 2005) . . . . .	5
Figure 2.2	Effect of fiber content on the energy absorption capacity (Anbuvelan 2014) . . . . .	5
Figure 2.3	a) Schematic load-deflection diagrams of FRC with high volume fraction (Moghimi 2014) b) Typical load-deflection curves of FRC beams with low volume fraction (Fanella and Naaman 1985) . . . . .	7
Figure 2.4	Experimentally observed load-deflection curves of steel and polypropylene fiber reinforced concrete beams (Fanella and Naaman 1985) . . . . .	8
Figure 2.5	Experimentally observed load-deflection curves for different types of fibers (Fanella and Naaman 1985) . . . . .	8
Figure 2.6	Chemical structure of polypropylene (Moghimi 2014) . . . . .	10
Figure 2.7	Synthetic fibers . . . . .	10
Figure 2.8	Steel fiber geometries (Daniel, Gopalaratnam and Galinat 1999) . . . . .	13
Figure 2.9	Stress-strain curves for steel fiber reinforced concrete under compression (Moghimi 2014). . . . .	15
Figure 2.10	Variation of splitting tensile strength with Fiber content (Ramujee 2013) . . . . .	18
Figure 2.11	Comparison of load-deflection curves (Hameed 2009) . . . . .	21
Figure 2.12	Relation between initial modulus of elasticity and percentile of fiber (Mohamed 2006). . . . .	22

Figure 2.13 Plan view of suggested method of deflection measurement. . . . .	26
Figure 2.14 Suggested method of deflection measurement to exclude load-train and crushing of concrete at the point of loading using a linear variable deflection transducer (LDVT). . . . .	26
Figure 2.15 ENI14488-5 testing on steel support (Rivaz 2015). . . . .	28
Figure 2.16 Set-up for plate test (EFNARC 1996). . . . .	28
Figure 3.1 Polypropylene fiber used . . . . .	35
Figure 3.2 The gradation of aggregates. . . . .	36
Figure 3.3 Square and round panel molds W: Width, L: Length, h: Height, D: Diameter. . . . .	37
Figure 3.4 MTS testing machine . . . . .	39
Figure 3.5 Base plates of the two plate specimens . . . . .	39
Figure 3.6 Engine crane . . . . .	39
Figure 3.7 A general view of the specimens in the laboratory . . . . .	40
Figure 3.8 The two types of specimen tested a) Square panel b) Round panel .	41
Figure 3.9 Typical force-deflection graph of a square panel . . . . .	42
Figure 3.10 Typical energy-deflection graph of a square panel . . . . .	43
Figure 3.11 Typical force-deflection graph obtained from round plate specimen measured from piston and LVDT . . . . .	43
Figure 4.1 a) Slump and b) Slump flow of fresh concrete. . . . .	46
Figure 4.2 Force deflection graph and crack pattern of NPFC 3 square panel samples . . . . .	47

Figure 4.3 Force deflection graph and crack pattern of NPFC 6 square panel samples . . . . .	48
Figure 4.4 Force deflection graph and crack pattern of NPFC 9 square panel samples . . . . .	49
Figure 4.5 Force deflection graph of NPFC 3, 6, 9 square panel samples . . . . .	50
Figure 4.6 Force deflection graph and crack pattern of HPFC 12 square panel samples . . . . .	51
Figure 4.7 Force deflection graph and crack pattern of HPFC 18 square panel samples . . . . .	52
Figure 4.8 Force deflection graph of HPFC 24 square panel samples . . . . .	53
Figure 4.9 Force deflection graph of HPFC 12, 18, 24 square sampels . . . . .	54
Figure 4.10 Comparison of NPFC and HPFC square samples . . . . .	55
Figure 4.11 Energy deflection comparison of all square panel samples . . . . .	56
Figure 4.12 Energy vs. fiber volume fraction of square panels . . . . .	57
Figure 4.13 Force deflection graph and crack pattern of NPFC 3 round panel samples . . . . .	59
Figure 4.14 Force deflection graph and crack pattern of NPFC 6 round panel samples . . . . .	60
Figure 4.15 Force deflection graph and crack pattern of NPFC 9 round panel samples . . . . .	61
Figure 4.16 Force deflection graph of NPFC 3, 6, 9 round panel samples . . . . .	62
Figure 4.17 Force deflection graph and crack pattern of HPFC 12 round panel samples . . . . .	63
Figure 4.18 Force deflection graph and crack pattern of HPFC 18 round panel samples . . . . .	64

Figure 4.19 Force deflection graph of HPFC 24 round panel sample . . . . .	65
Figure 4.20 Force deflection graph of HPFC 12, 18, 24 round panel samples . .	66
Figure 4.21 Comparison of NPFC and HPFC round samples . . . . .	67
Figure 4.22 The Energy vs. deflection comparison of all round panel samples. .	67
Figure 4.23 Energy vs. fiber volume fraction of round panels . . . . .	68
Figure 4.24 Relationship of energy obtained from square and round panel tests	69

## LIST OF ABBREVIATIONS

NPFC	Normal Dosage Polypropylene Fiber Concrete
HPFC	High Dosage Polypropylene Fiber Concrete
ACI	American Concrete Institute
ASTM	American Society for Testing and Materials
BS	British Standard
EN	European Norms (European Standards)
NBN	Belgium National Standards “Bureau voor Normalisatie/Bureau de Normalisation “
FRC	Fiber Reinforced Concrete
$V_f$	Volume Fraction (%)
LVDT	Linear Variable Differential Transformer
PC	Portland Cement
SF	Silica Fume
FA	Fly Ash
W	Water
SP	Super Plasticizer
METU	Middle East Technical University
MTS	Loading Frame Brand, Material Testing System

# CHAPTER 1

## INTRODUCTION

### 1.1 General

With the developing technology in material science, the usage areas of synthetic fibers have been expanded. Especially in construction field, synthetic fibers such as polyacrilics, aramid (Kevlar), carbon (Pan), polyester, polyethylene, polyolefins and polypropylene are now actively being utilized. The addition of fibers to concrete enhances the its mechanical properties in different ways. In order to evaluate this enhancement, there are many test procedures defined in different standards and guides according to the performance criteria intended to be measured.

Considering that the main aim of fiber addition is to enhance the flexural performance of concrete, flexural tests such as bending and central point loading plate tests are the most commonly used tests to measure this enhancement. On the other side, since the normal use of synthetic fibers in concrete does not mainly improve the tensile or the flexural strength, determining the enhancement in the toughness or the energy absorption capacity is more suitable. In this scope, there are two main test methods, which are bending and panel tests, commonly used for this purpose. These methods generally use the load deformation curves obtained from the test to calculate the energy absorption capacity of the specimen.

## 1.2 Scope and Objective

There are not so many studies available in the literature with high dosage synthetic fibers such amount of 12, 18 and 24 kg/m<sup>3</sup> corresponding to volume fractions of 1.32%, 1.67%, 2.64%. Therefore, to compare the behavior of higher dosages of synthetic fibers with normal dosages 3, 6 and 9 kg/m<sup>3</sup> in fiber reinforced concrete, the study was conducted under different test methods.

In this study, two test methods were utilized both for centrally loaded plates; ASTM 1550 for round plates and EFNARC for square plates. They were used to investigate the effect of different amount of synthetic fiber additions to concrete. The amount of additions were considered under two main parts. The first one is what is usually used and recommended in practice as minimum, moderate and maximum dosages (3, 6 and 9 kg/m<sup>3</sup>). The second one, is high dosage of synthetic fibers, that usually unable to be used with conventional concrete (12, 18 and 24 kg/m<sup>3</sup>). The tests were conducted on specimens prepared from the different synthetic fiber reinforced concrete mixtures. The energy absorption capacity for each plate of each mixture and plate shape were determined for a deflection up to 25 mm. In addition to that, a comparison between the results of the two test methods were made in order to determine the relationship between them.

This study consist of five chapters. The first chapter contains a general summary about the thesis topic and states the objective of the performed work. The second chapter contains a literature review about the fibers used in concrete, the properties enhanced by this use, the methods used to measure this enhancement and the test methods used in this study. In the third chapter, the properties of the materials used in the production of the test specimens, along with the production methods were explained. Moreover, the procedures of the applied tests and the test analyzing methods were also explained in that chapter. The test results obtained in this study together with discussion about those are included in Chapter four. Finally, the conclusions of this work followed by some recommendations about possible related future work are presented in Chapter five.

## CHAPTER 2

### LITERATURE REVIEW

Fiber reinforced concrete is a composite material which is apart from plain concrete on the basis of its constituents that give the concrete some unique properties by adding some fibrous materials which increase its structural integrity. A remarkable innovation in concrete technology was achieved by the utilization of fibers to reinforce the concrete (Abbas and Khan 2016).

#### 2.1 Historical Use of Fibers

Over the past years, several different materials have been used as a fiber reinforcement to increase the volume stability and mechanical properties of construction materials by enhancing the post-cracking behavior. Before Christ (B.C) horse hair was used as fiber (Jain and Kothari 2012). At about the same time period, approximately 3500 years ago, sun-baked bricks reinforced with straws were used to build the 57 m high hill of Aqar Quf (near Baghdad). In about 1900s with the invention of Hetschek, the asbestos fibers were developed (Bentur and Mindess 2007). The steel and glass fibers were used in the early work on Fiber Reinforced Concrete in the 1950s and 1960s. Since then, with the continuous developing technology and scientific innovations, various types of fibers were used to reinforce many different materials.

#### 2.2 Definition of Toughness

Brittle materials like concrete do not show a ductile behavior at the stage of post-cracking. These non-reinforced materials, initially deform elastically. This elastic deformation is

followed by micro cracking, localized macro cracking and then fracture. However, with the addition of fibrous materials into the concrete post-elastic property is enhanced and the deformation capacity under the load after post-cracking is enhanced as well (ACI 2012). Abbas and Khan stated that the fiber reinforcement can alter the brittleness of concrete by increasing the toughness (FHA 2005). At this point, the term of “energy absorption capacity”, on the other name “toughness” come into prominence.

In the literature, the toughness of concrete is identified as:

- The total energy absorbed prior to complete separation of the specimen which is given by the area under load deflection curve (Wafa 1990).
- According the ACI Report (Shah and Daniel 1999), under the effect of dynamic or impact loads or static strains, the measure of capability of resistance to fracture defines the toughness of the materials.
- The property that needs to be used in determining the load carrying capacity of fiber reinforced concrete under deflection (Scanfibre n.d.).
- Toughness means energy absorption capability of hardened concrete resulting in improved deformability (Ceylan 2014).
- Toughness is generally recognized as the property most enhanced by the addition of fiber reinforcement to concrete (Robins, Austin and Peaston 1989).
- Toughness can represent the energy absorbing ability of the material, and can be used to determine the resistance to the fracture under loading condition (Mao and Barnett 2017).

The graph in Figure 2.1, demonstrates how the load-deflection curves are changing with the fiber types. Without fibers, after the initial crack the specimen has no more load carrying capacity. However, with the addition of fibers, which are seen on the graph such as Fiber A, Fiber B and Fiber C, the specimen has extended load bearing

capacity after the initial crack. The area under the load-deflection graph is changing with the different indicative fiber types. That means the toughness of concrete depends on the fiber properties as well. The factors affecting the toughness will be described in the following sections.

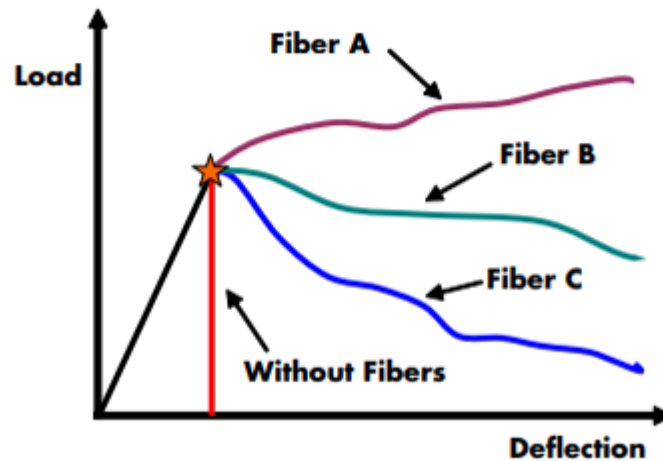


Figure 2.1: Effect of fiber type in toughness (FHA 2005)

As seen in Figure 2.2, the stress vs. strain curve of the high fiber volume reinforced, low fiber reinforced and plain concrete are compared. According to the graph, with the addition of fiber, the strain can be extended by increasing the energy absorption capacity of concrete. The plain concrete's stress is decreasing suddenly on a certain point where it has reached its maximum strain. However, with the addition of fiber, the stress decreases gradually with the greater range of strain considerably.

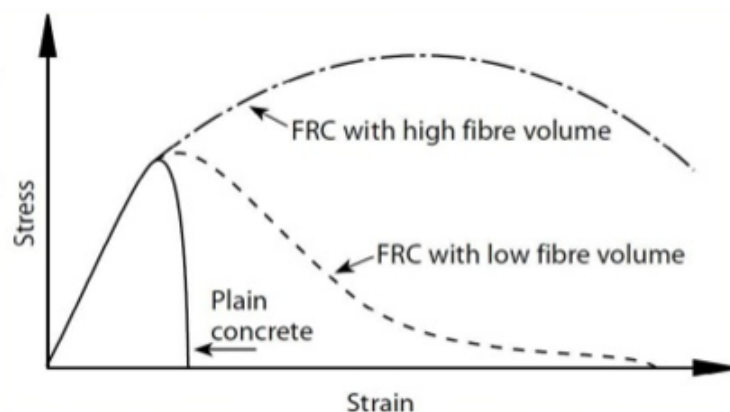


Figure 2.2: Effect of fiber content on the energy absorption capacity (Anbuvelan 2014)

### 2.2.1 Load-Deflection Response of Fiber Reinforced Concrete

Figure 2.3, shows the load – deflection response of a typical fiber reinforced concrete specimen which is tested under flexure. There are three stages in this graph;

- Up to point A, the more or less linear response can be seen. This range can be named as elastic response stage of the fiber reinforced concrete. In this portion, a strengthening mechanism behavior which involves a transfer of stress from the matrix to the fibers. The matrix and the fibers share the imposed stress until the first initiation of cracks occurred which is termed as “First cracking strength” or "Proportional Limit",
- Between A and B is a non-linear portion of the graph. In this portion, and after cracking, the stress continuously transferred from the matrix to the fibers. With the increase of load, the fibers have the tendency of slightly pulling out from the matrix which leads to a non-linear load deflection response until the maximum load capacity, with the other name “peak strength”, is reached. The strain hardening behavior starts here and continues in the following stages,
- The portion starting from point B continues until complete failure. A loss in strength is encountered with increasing the deformation. This stage is an important indicative sign that the fiber composite can absorb energy before the failure. This characteristic is referred as “toughness”.

The load-deflection behavior as in Figure 2.3a, can be seen only if an adequate amount of volume fractions of fiber exists. Even after first crack occurs, the strain hardening process allows an increase in load that means Load-B is greater than Load-A. For lower volume fractions the ultimate strength intersects with first cracking strength and the load deflection curve starts to decrease suddenly as it can be seen in the Figure 2.3b.

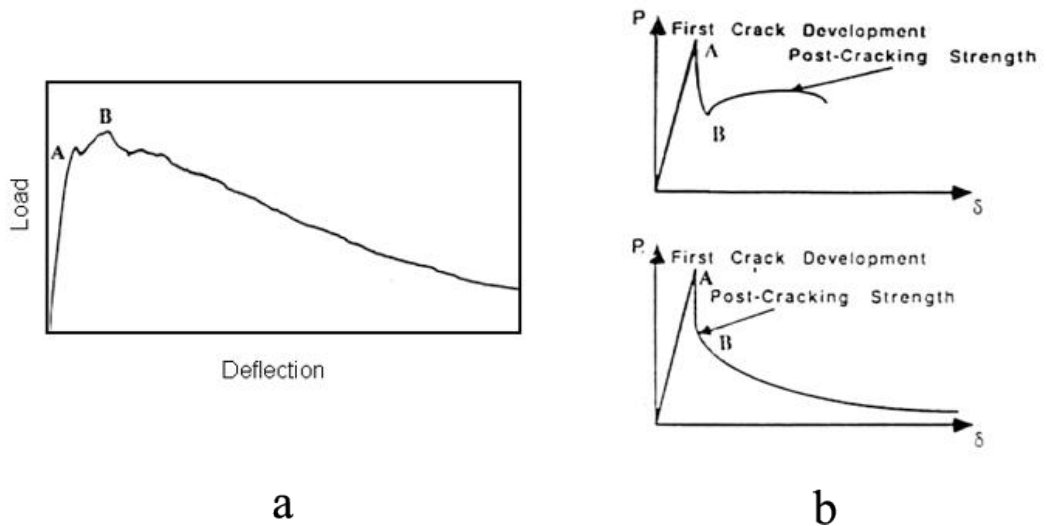


Figure 2.3: a) Schematic load-deflection diagrams of FRC with high volume fraction (Moghimi 2014) b) Typical load-deflection curves of FRC beams with low volume fraction (Fanella and Naaman 1985)

### 2.3 Fiber Types

Nowadays, there are various types of cementitious composites with different fibers. The most commonly used fiber types are: steel fibers, glass fibers, asbestos fibers, synthetic fibers and natural fibers (UDT 1994).

Typical load-deflection curves of FRC beams observed experimentally for different types of fibers are shown in Figures 2.4 and 2.5.

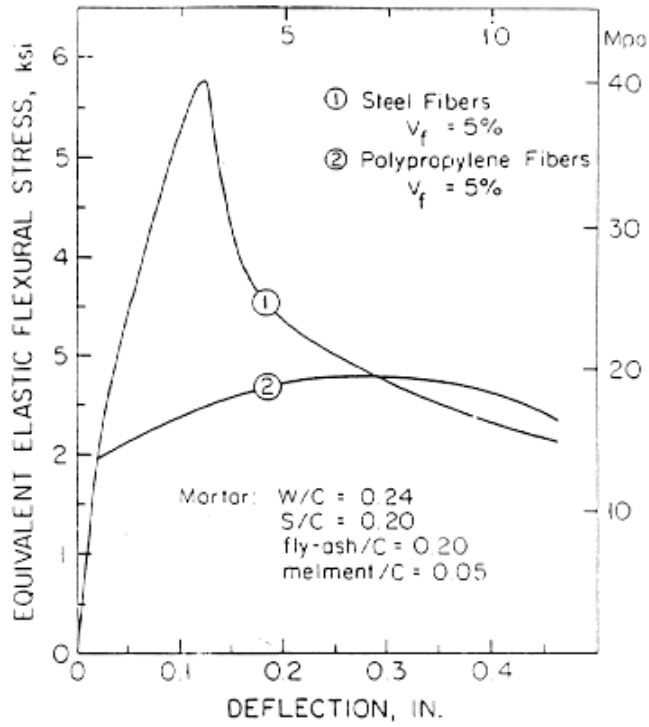


Figure 2.4: Experimentally observed load-deflection curves of steel and polypropylene fiber reinforced concrete beams (Fanella and Naaman 1985)

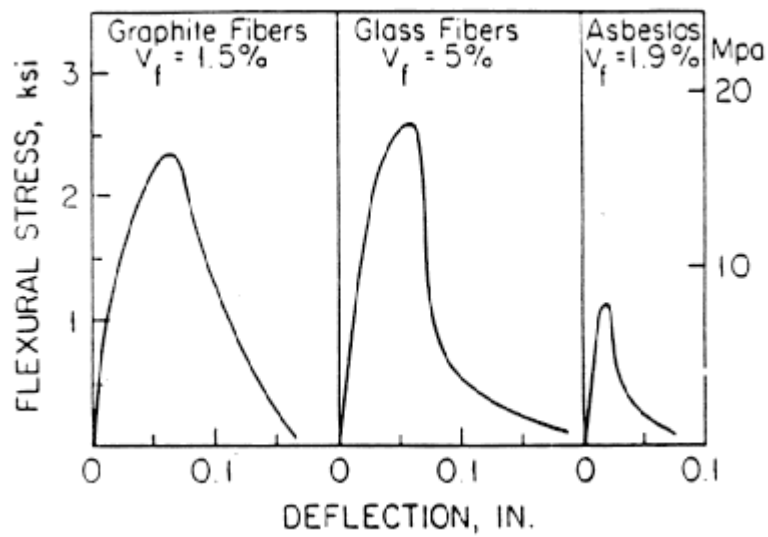


Figure 2.5: Experimentally observed load-deflection curves for different types of fibers (Fanella and Naaman 1985)

### 2.3.1 Synthetic Fibers

Synthetic fibers, or polymer fibers, are extensively used in various structural elements. These fibers are made from synthesized polymers of small molecules, where raw materials such as petroleum based chemicals or petrochemicals are used.

In a cementitious composites, the most commonly used synthetic fiber types are: Polyacriliacs, aramid (Kevlar), carbon (Pan), polyester, polyethylene, polyolefins, polypropylene.

Carbon fibers among which most commonly used in construction industry are Pitch and Pan type carbon fibers. Pitch carbon fibers are based on coal tar and petroleum products while pan carbon fibers based on Polyacrylonitrile. Due to its high tensile strength, for structural reinforcement most common used one between them is pan carbon fibers.

Some typical properties of synthetic fibers; such as diameter, specific gravity, tensile strength, elastic modulus and ultimate elongation are listed in Table 2.1.

Table 2.1: Typical properties of synthetic fibres (Bentur and Mindess 2007)

Fiber Type	Diameter $\mu\text{m}$	Specific Gravity	Tensile Strength (GPa)	Elastic Modulus (GPa)	Ultimate Elongation %
Acrylic	20-350	1.16-1.18	0.2-1.0	14-19	10-50
Aramid (Kevlar)	10-12	1.44	2.3-3.5	63-120	2-4.5
Carbon (PAN)	8-9	1.6-1.7	2.5-4.0	230-380	0.5-1.5
Carbon (Pitch)	9-18	1.6-1.21	0.5-3.1	30-480	0.5-2.4
Nylon	23-400	1.14	0.75-1.0	4.1-5.2	16-20
Polyester	10-200	1.34-1.39	0.23-1.2	10-18	10-50
Polyethylene	25-1000	0.92-0.96	0.08-0.60	5	3-100
Polyolefin	150-635	0.91	275	2.7	15
Polypropylene	20-400	0.9-0.95	0.45-0.76	3.5-10	15-25
PVA	14-650	1.3	0.8-1.5	29-36	5.7
Steel (for comparison)	100-1000	7.84	0.5-2.6	210	0.5-3.5
Cement matrix	-	1.5-2.5	0.003-0.007	10-45	0.02
Note: The values in the table are for fibers that are commercially available. They may vary considerably from manufacturer to manufacturer.					

### 2.3.1.1 Polypropylene Fibers Used in This Study

In this thesis study, the polypropylene fibers were used as a fiber reinforcement. Therefore among the synthetic fibers, only this type will be described.

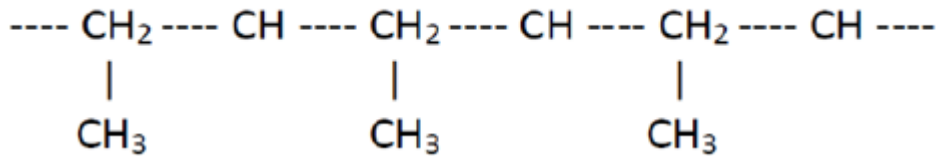


Figure 2.6: Chemical structure of polypropylene (Moghimi 2014)

Polypropylene fibers have a lower specific gravity, therefore they are considered as a lightweight material compared to other fibers which are used in the concrete as a fiber reinforcement. They also have a low modulus of elasticity as shown in Figure 2.1.

Polypropylene is a hydrophobic material; therefore, it does not absorb water. It's fibers do not show a chemical bonding reaction with any constituents of concrete, the only bonding can be ensured by mechanical ways (ACI 2012).

The fibers are produced either by the pulling wire procedure with circular cross section or by extruding the plastic film with rectangular cross-section. As a result of this manufacturing, the consequence comes to exist as fibrillated bundles, mono filament or microfilaments. Examples of these products can be seen in Figure 2.7.



Figure 2.7: Synthetic fibers

As a result of extrusion process in which the polypropylene resin is hot drawn through a die, mono filament polypropylene fibers are produced. The diameters of mono filaments vary between 0.05 mm to 0.20 mm (Bentur and Mindess 2007).

On the other hand, by expanding a plastic film and then by separating it into strips and with a final slit process, fibrillated polypropylene fibers are formed. The fibrillated fiber bundles are cut into the desired length.

To quantify the geometry of fibrillated polypropylene fibers is difficult. Therefore, fibrillated geometry can be examined by adsorption techniques with the measurement of specific surface area (Bentur and Mindess 2007).

Although mono filament and fibrillated polypropylene fibers have almost the same strength and elastic modulus, in the scope of the capability of holding cracks, mono filament fibers give better results than fibrillated fibers (Singh, 2011).

Polypropylene fibers are commonly used for two purposes in the cementitious matrices. The first one is as primary reinforcement in thin sheet components with the high volume content as high as 5% by volume to ensure both strengthening and toughness properties of concrete. The other application is based on the purpose of using it as a secondary reinforcement for crack control. In this situation, the volume content of polypropylene is lower than the previous one which is about less than 3% by volume. Such a low volume may not be suitable for structural and load bearing applications, but it can enhance the structural stability (Singh, 2011).

Table 2.2: Properties of various types of polypropylene fibers (Singh, 2011)

<i>Fiber Type</i>	<i>Length (mm)</i>	<i>Diameter (mm)</i>	<i>Tensile Strength (MPa)</i>	<i>Modulus of Elasticity (GPa)</i>	<i>Specific Surface (m<sup>2</sup>/kg)</i>	<i>Density (kg/cm<sup>3</sup>)</i>
Monofilament	30-50	0.30-0.35	547-658	3.50-7.50	91	0,9
Microfilament	12-20	0.05-0.20	330-414	3.70-5.50	225	0,91
Fibrillated	19-40	0.20-0.30	500-750	5.00-10.00	58	0,95
Modified Olefin	48	0,90-0,92	640	10		0,91

### **2.3.1.2 Modified Olefin**

In this thesis study, modified olefin polypropylene fibers were used. Olefin fiber is a synthetic fiber made from a polyolefin, such as polypropylene or polyethylene. With the addition of photoinitiators and with the help of co-additions which are one or more double bonds, the polymers are modified. As a result of this process, the tensile strength as well as the modulus of elasticity of fibers is increased (Ezeldin and Lowe 1991). Compared to the steel fibers, the durability of modified olefin fibers are better especially in rust resistance and anti-spelling properties (ACI 1999).

### **2.3.2 Steel Fibers**

The high modulus of elasticity, which the steel fibers have, provides a considerable structural durability on the concrete by bridging the micro cracks. The bridging effect starts when the first crack appears. Because the modulus of elasticity and the strength of steel fibers are higher than concrete matrix, the fibers start to resist crack propagation. Besides that, the non-uniform distribution of steel fibers supports the structural geometry in three dimension. This three dimensional support enhances the structural durability after the first crack appeared. Like the spider network, non-uniform distribution prevent crack progression as much as possible in any type of crack geometry compared to the plain concrete. If the fibers were aligned for example in one regular direction, the crack propagation of the transverse direction would not affected like in plain concrete. Therefore, the nonuniformity in fibers allows an increase of toughness.

Steel fiber reinforced concrete fails only after the steel fiber breaks or is pulled out of the cement matrix. When the first crack appears, the fibers start to resist to the stress and some amount of stress is consumed by fibers until the fiber breaks. However, in pulling out case, the energy that one fiber can absorb up to the best of its ability is not met as in the case of breaking, therefore; it ends up without reaching its maximum resisting capacity.

The types of steel fibers are classified by ASTM A820 as:

- Type-1 : Cold-Drawn wire
- Type-2 : Cut Sheet
- Type-3 : Melt-Extracted
- Type-4 : Mill Cut
- Type-5 : Modified Cold-Drawn Wire

Also , there are different types of steel geometries which are commercially available to use in steel fiber reinforced concretes as seen in Figure 2.8 below.

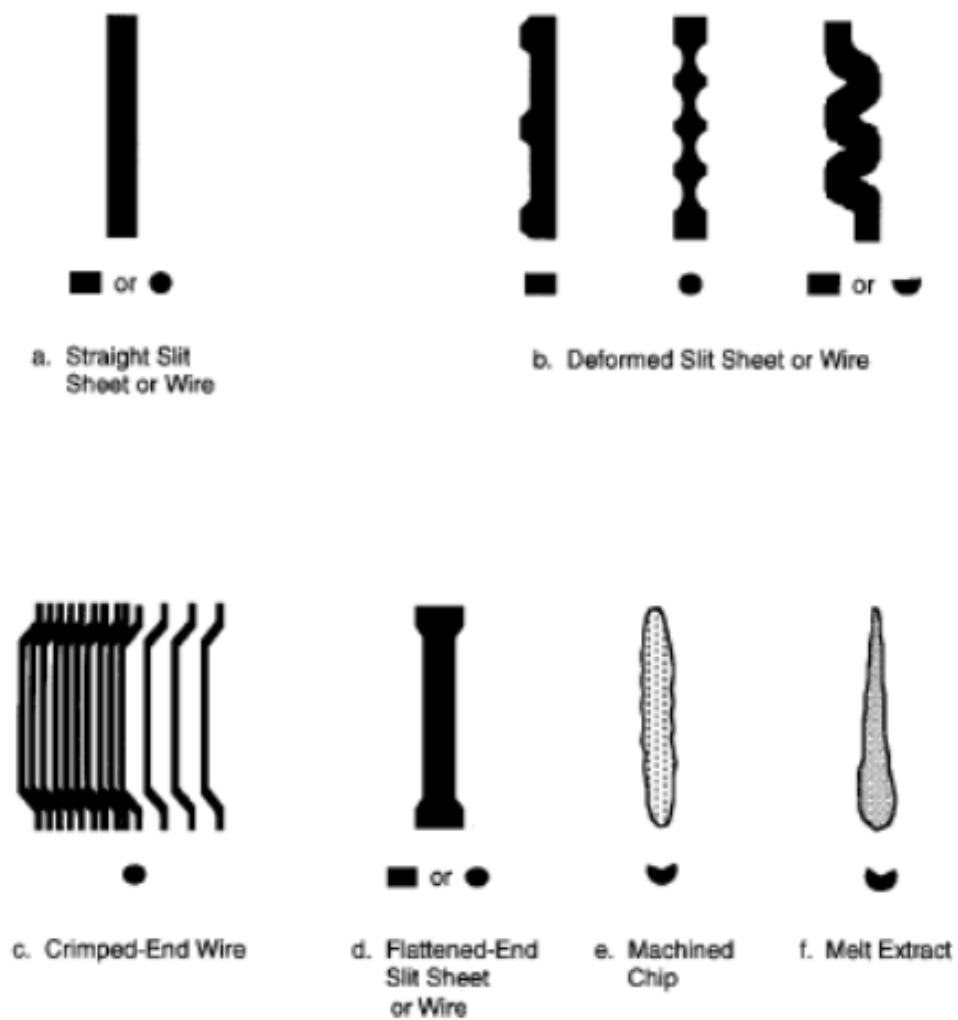


Figure 2.8: Steel fiber geometries (Daniel, Gopalaratnam and Galinat 1999)

Round, straight steel fibers are produced by cutting or chopping wires, which have the diameter of 0.25 to 1.00 mm. Flat, straight steel fibers having a typical cross section ranging from 0.15 to 0.64 mm.

The typical aspect ratio of steel fibers are ranging from 20 to 100 while length dimensions ranging 6.4 to 76 mm (Daniel, Gopalaratnam and Galinat 1999).

## 2.4 Mechanical Characteristics of Fiber Reinforced Concrete

It is known that several properties of FRC are affected by the use of fibers. For example, the summarized properties of concrete that are affected by steel fibers are shown in the Table 2.3.

In this thesis study, the main mechanical property which has been investigated that with the changing fiber dosages determining the energy absorption capacity of polypropylene fiber reinforced concrete by using ASTM C-155 Round Panel Test and EFNARC Square Panel Test Methods (ASTM C1550; EFNARC 1996).

Table 2.3: The performance of steel fiber reinforced concrete compared to unreinforced concrete (Bothma 2013)

Property	Comment
Abrasion resistance	Improvement may be achieved as a result of reduced bleeding.
Compressive strength	Little change.
Electrical resistance	No significant change at fibre dosages generally used.
Fatigue resistance	Improvements even at low dosages.
Flexural strength	Little change in first crack strength at dosage rates commonly used.
Freeze-thaw resistance	Can reduce the deterioration caused by freeze-thaw cycling.
Impact resistance	Major improvements.
Modulus of elasticity	No significant change at fibre dosages generally used.
Restrained shrinkage	Even at low dosages, better distribution of stresses can reduce crack widths.
Shear strength	Improvements even at low dosages can be achieved in combination with reinforcing bars.
Spalling resistance	Being dispersed throughout the matrix, steel fibre reinforcement gives superior protection to exposed areas such as the joint arris.
Thermal shock resistance	As with impact resistance, there are improvements even at low dosage rates, a typical application being foundry floors.
Toughness	Major improvements, even at low dosages.

### 2.4.1 Compressive Strength

As a result of several researches related to the compressive strength in the presence of fiber reinforcement in concrete composite structures, it can be concluded that the addition of fiber to the concrete matrix has negligible effect on the compressive strength. This is generally because of the fact that compressive strength decreases highly after the first crack occurrence and any stress bridging after that has a small contribution to the compressive strength. However, the compressive strength of polypropylene fiber reinforced concrete is affected by higher percentage of polypropylene fibers at about 5% (Moghimi 2014).

In ACI Committee 544, “Measurements of properties of fiber reinforced concrete”, ACI Material Journal, Vol. 85, No. 6, 1988, pp. 583-593, it is stated that the addition of fibers to the concrete has a little or no effect on the compressive strength and the modulus of elasticity. As shown on Figure 2.9, there is no significant change in compressive stress when fibers are used (Bentur and Mindess 2007; Moghimi 2014).

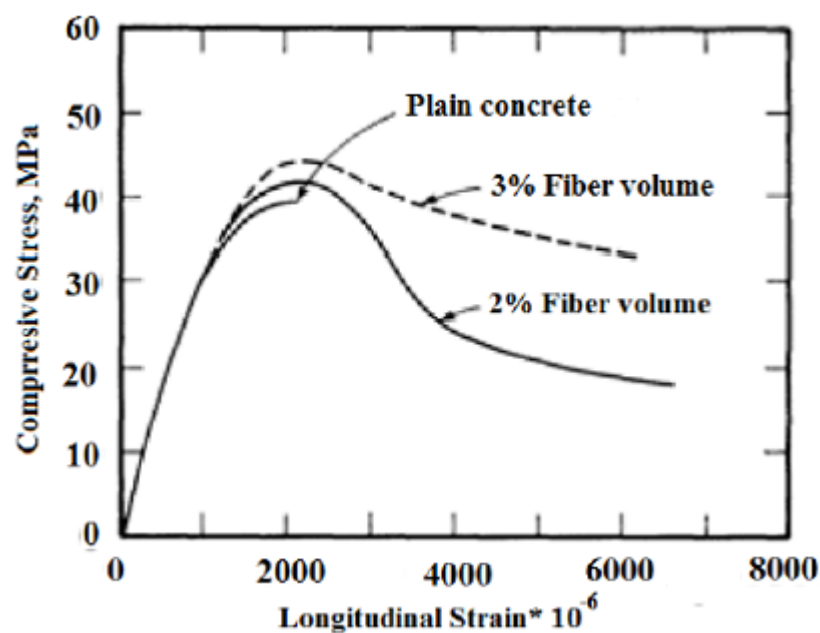


Figure 2.9: Stress-strain curves for steel fiber reinforced concrete under compression (Moghimi 2014).

## 2.4.2 Flexural Strength

The flexural strength of fiber reinforced concrete depends on the volume fraction and the tensile and bond strengths of the fibers. The longer the fiber, the better the bond strength (Bothma 2013). An ideal fiber to boost the modulus of rupture would be a long fiber that has higher tensile and bond strengths. At low dosages of fiber volume fractions, there is no considerable increase in the flexural strength of the concrete. To attain significant improvements, higher fiber volume fraction should be used. A study showed that, 38.1 mm monofilament polypropylene fiber increased the modulus of rupture due to the high tensile strength fiber effect.

Alhozaimy et.al (1995) performed an experiment on polypropylene fiber reinforced concrete by applying flexural strength test. They pointed out that flexural toughness is increased by 44% and 386% respectively for the volume of fractions 0.1% and 0.3% compared to plain unreinforced concrete for the same mix design (Bothma 2013). The Table 2.4 shows that how modulus of rupture changes with the changing fiber volume fraction.

Table 2.4: Modulus of rupture of changing fiber volume fraction (Bothma 2013).

Mix	Modulus of Rupture (MPa)	Fiber Volume Fraction (%)
M01	3.55	0
M02	3.58	0.1
M03	4.30	0.1
M04	3.82	0.1
M05	4.24	0.1
M06	3.96	0.1
M07	4.65	0.1
M08	4.24	0.1
M09	4.07	0.3
M10	4.27	0.3

### **2.4.3 Modulus of Elasticity**

Experimental studies (Fanella and Naaman 1985; Shah et al. 1978) have shown that the addition of fibers have a slight effect only on the modulus of elasticity of the stress-strain curve of the composite.

In an experiment carried out by Ezeldin and Lowe (1991), the steel fibers in different volume fraction was used (30, 45 and 60 kg/m<sup>3</sup>) with concrete strengths varying from 35 to 85 MPa to report the secant modulus of elasticity under compression. It was reported that with the increasing steel fiber volume fraction, the increase in modulus of elasticity was considerable (Ezeldin and Lowe 1991).

### **2.4.4 Splitting Tensile Strength**

Bentur (2007), Hasan et al. (2011), Roesler et al. (2006) have found that, for the direct tensile strength of concrete, polypropylene fibers has not shown a considerable effect, but for the splitting tensile strength, the addition of macro-synthetic polypropylene fibers provides an increase the strength increase in the splitting tensile strength (Mohod 2015).

Ramujee carried out an experiment with different volume percentages of polypropylene fibers in 12 mm length, circular cross section. As it can be seen on Figure 2.10, there is an optimum amount of fiber volume fraction that can give a maximum splitting tensile strength. Compared to the non-fiber reinforced concrete, the maximum splitting tensile strength increase is 40% at 1.5% by volume fiber content. Therefore it can be said that optimum value of this study of splitting tensile strength is 1.5% fiber content (Ramujee 2013).

Tavakoli has performed a study on tensile and compressive strengths of polypropylene fiber reinforced concrete. The polypropylene fibers used were 7 cm in length, with an aspect ratio of 50, and the modulus of elasticity of  $25 \times 10^3$  MPa. As a result of this experiment it was seen that the ultimate tensile strength and strain both increases with increasing fiber ratio. That leads to an increase in ductility of concrete. However, it

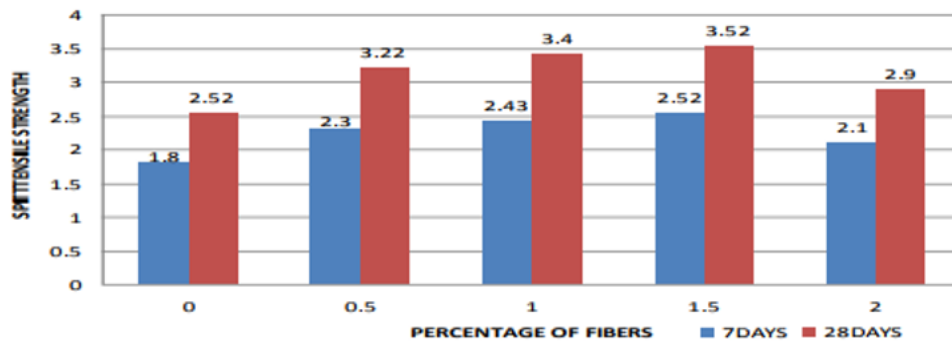


Figure 2.10: Variation of splitting tensile strength with Fiber content (Ramujee 2013)

was also noted that a fiber volume fraction which is higher than 1.5% leads to strain decrease. It was reported as a conclusion that tensile strength of concrete increases about 80% with the use of 1.5% polypropylene fiber by volume (Tavakoli 1994).

#### 2.4.5 Impact Resistance

The impact resistance of normal unreinforced concrete may not reach desirable levels. With the addition of fiber, the impact resistance of concrete increases considerably.

Bentur et.al (1989) performed a study on impact resistance of polypropylene fiber reinforced concrete. They found out that in both high and normal strength concrete, the addition of polypropylene fibers with low volumes between 0.1% to 0.5% have only a small positive influence on the impact resistance of concrete (Anbuvelan 2014).

On the contrary, Chu et. al (1989) carried out in their study a test on the impact resistance of small concrete beams with polypropylene fiber. They reported that with the polypropylene fibers in concrete, the impact resistance has increased by 29% (Anbuvelan 2014).

In another study carried out by Anbuvelan, ACI Drop Weight Impact tests were performed. The drop hammer was dropped recurrently and then the numbers of blows required for the first visible crack to form at the top surface and for ultimate failure to occur were reported (Anbuvelan 2014).

In that study, they used the concrete strengths (M1:21 MPa, M2: 32 MPa, M3: 48 MPa) and utilized three fiber dosages (0.1%, 0.2% and 0.3%) as shown in Table 2.5. The results of that study, shows that the addition of fibers increases the impact resistance of concrete for different concrete strength values (Anbuvelan 2014).

Table 2.5: Impact strength test results (Anbuvelan 2014).

No	Dosage of Fiber in Concrete %	No. of blows for first crack (Ave. of 5 specimens)	No. of blows for ultimate strength (Ave. of 5 specimens)
M1 (21MPa)	0.0	348	368
	0.1	400	425
	0.2	437	482
	0.3	493	537
M2 (32MPa)	0.0	448	510
	0.1	493	552
	0.2	558	622
	0.3	490	551
M3 (48MPa)	0.0	624	691
	0.1	705	796
	0.2	945	1015
	0.3	1059	1204

## **2.5 Fiber Properties Affecting Mechanical Characteristics of FRC Concrete**

According to the “State of the Art Report on Fiber Reinforced Concrete “ by ACI Committee 544, test data which have been obtained from composite concrete samples containing polypropylene fibers at volume percentages ranging from 0.1 to 10.0 percent, it has been reported that the properties of the composites are greatly affected by the volume, geometry, length, modulus, aspect ratio, strength, surface bonding characteristic of the fiber, and the production method, the composition matrix, the strength of the matrix. This is also valid for all the other synthetic fiber types (ACI 2012).

### **2.5.1 Fiber Aspect Ratio**

Aspect ratio can be defined as the ratio of fiber length to its diameter (Kalpakjian and Schmid 2001). The effect of the aspect ratio of fibers is also related to “the critical fiber length”, which can be defined as the minimum length of the fiber that allows the development of sufficient stress to cause the fiber to fail at its midpoint. The interfacial fracture energy of the adhesive interface between the fibers and the matrix versus the tensile strength of the fiber has an impact on the critical fiber length. It has been concluded that for advanced FRCs, the critical fiber length could be as much as 50 times the diameter of the fiber. To eliminate the fiber debonding under tensile stress, FRCs with longer fibers could exhibit strength similar to the corresponding continuous FRC (Valittu 2015).

According to the “State of the Art Report on Fiber Reinforced Concrete“ reported by ACI Committee 544, high aspect ratio fibers show more effective behavior in enhancing the post-cracking behavior of fiber reinforced concrete. This is caused by high resistance to pull-out from the matrix. However, the balling of the high aspect ratio fibers during the mixture stage is a drawback. To ensure the high pull-out resistance without allowing balling while reducing fiber aspect ratio, enlarging or hooking the ends of the fibers and roughening their surface texture are some useful methods.

Hameed et. al. (2009), carried out an experimental study to investigate the effect of fiber aspect ratio on load bearing capacity, post-crack strength and flexural toughness of fiber concrete mixture. In this test, high performance metallic fibers have been used in different aspect ratios (20 mm and 30 mm in length with 105 and 125 aspect ratio respectively) while the dosage of fibers was kept constant at  $20 \text{ kg/m}^3$  (0.25% by volume fraction).

As it is seen from Figure 2.11 the peak load is reached by the M20F30 specimen which has the greatest fiber aspect ratio. Maximum Load carried by M20F30 was 80% more than the control concrete and 27% more than the M20F20 (Hameed 2009).

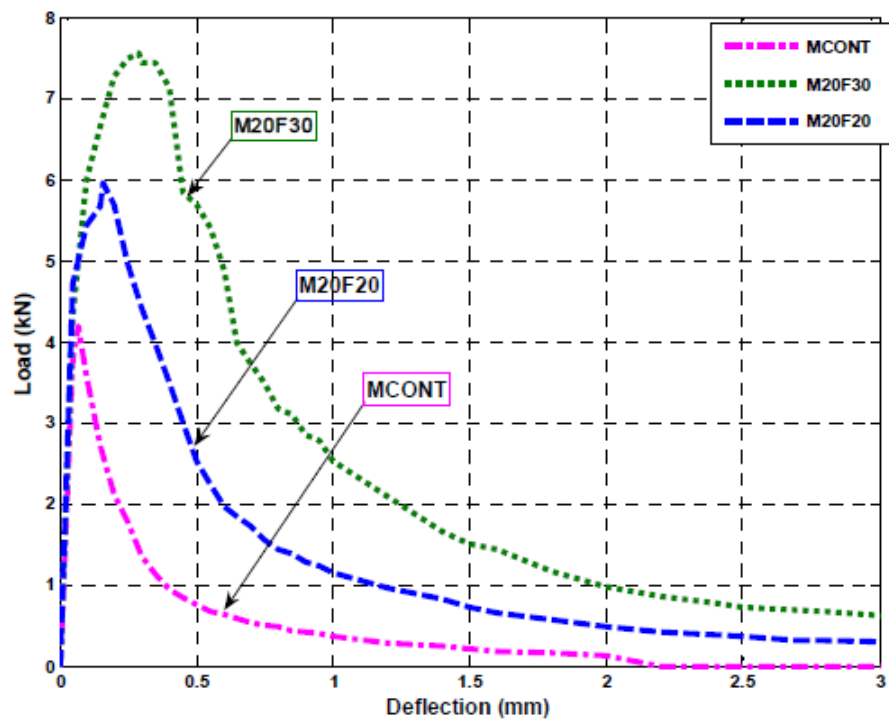


Figure 2.11: Comparison of load-deflection curves (Hameed 2009)

## 2.5.2 Concrete Matrix and Elastic Modulus of Fibers

Elastic modulus is the ratio between the applied stress and instantaneous strain within an assumed proportional limit. Elastic modulus, or Young's modulus, ( $E$ ), describes the stiffness of concrete. It is a function of the concrete's ingredients and their relative proportions.

Mohamed (2006), has carried out a work on polypropylene fiber reinforced concrete, where he observed that the initial  $E$  of the concrete has significantly reduced with increasing amount of polypropylene fibers, as can be seen from Figure 2.12.

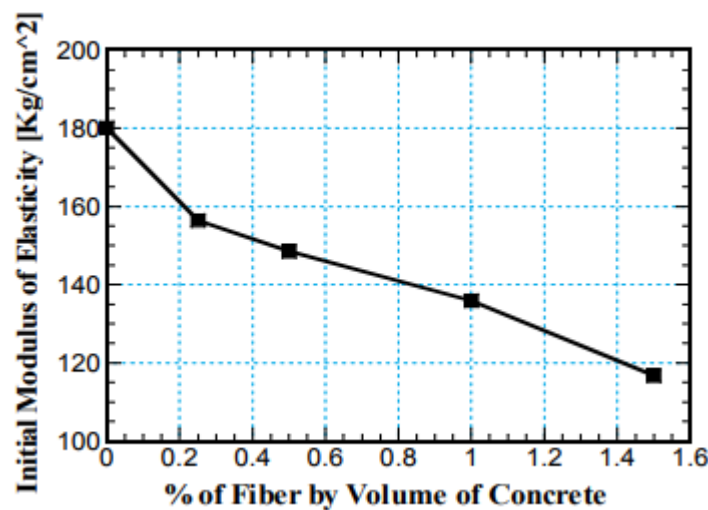


Figure 2.12: Relation between initial modulus of elasticity and percentile of fiber (Mohamed 2006).

To get the best performance of the fibers, they should have the ability to resist strains greater than the capacity of the concrete matrix. This can be related to the elastic modulus of the fiber and the matrix. The fibers have a small contribution during the pre-cracking phase of the concrete, however; through the post cracking their effect rises as they start to absorb the applied energy. Generally, the fibers do not take the loads until the first crack occurs in the concrete. This means that compressive and tensile strength of concrete are not affected by the addition of fibers of the cured concrete.

### **2.5.3 The Effect of Fiber Orientation, Geometry, Dispersion and Shape**

When fibers are added in sufficient amount, the bridging fibers share and transfer the load to the other side of the crack. When the subsequent transferring stage, multiple cracking occurs in the matrix. In the initiation of the cracking the fiber dispersion has an enormous role (Akkaya, Shah and Ankenman 2001).

One of the most important property that distinguish fiber reinforcement from the conventional steel rebar reinforcement is the orientation of the reinforcement. While conventional reinforcement can be oriented in desired direction, the fiber reinforcement are not always but ideally randomly distributed. It is stated that the fibers aligned parallel to the applied load provide more strength and toughness than randomly distributed or perpendicular fibers (Kumar et.al. 2015).

Microstructural studies verify that compared to the longer fibers, shorter fibers disperse better in the concrete matrix and thus, the toughness performance of the matrix is enhanced better.

Akkaya et.al. (2001) carried out an experiment on fiber reinforced extruded cement composites, and reported the post-peak behavior of the 2 mm and 6 mm long fibers which have an identical volume fraction of 3% for the same specimen sizes. They reported at the end of the experimental study that 2 mm long fibers exhibit a behavior which allows a post-peak property with enhanced multiple cracking but 6 mm long fibers did not exhibit multiple cracking.

According to the same study, it has been seen that the size and number of the fiber free areas and the clumping of the fibers play an important role on the energy absorption capacity of the concrete by affecting the cracking formation. When the fibers are clumping, there is an increase in the fiber free areas. Therefore, on this increased fiber free area, it is easy to move cracks in the matrix with the less energy requirement for the initiation and moving forward. Thus, clumping does not allow fibers to create a bridging behavior then the initial cracks advance through the matrix. Therefore it can be concluded as: the clumping and the volume fraction of fiber free areas in concrete

matrix affect the post-peak behavior of concrete negatively and this leads to a decrease in toughness of concrete.

Determining the dispersion and orientation of the fibers in the concrete matrix is a difficult process. Also, controlling the dispersion and orientation of fibers during the concrete mixing process is by no means an easy task.

## **2.6 Test Methods For Determining Flexural Toughness of Fiber Reinforced Concrete**

There are many different test methods used to determine the flexural strength of concrete specimens as listed below.

- ASTM C1018 : Standard Test Method for Flexural Toughness and First-Crack Strength of Fiber-Reinforced Concrete (Using Beam With Third-Point Loading)
  - ASTM C 293 : Standard Test Method for Flexural Strength of Concrete (Using Simple Beam With Center-Point Loading)
  - ASTM C1550 : Standard Test Method for Flexural Toughness of Fiber Reinforced Concrete (Using Centrally Loaded Round Panel)
  - BS EN 14488-5 : Testing sprayed concrete. Determination of energy absorption capacity of fibre reinforced slab specimens
  - EFNARC Square Panel Test Method
  - BS EN 14651 : Test method for metallic fibre concrete.
- Measuring the flexural tensile strength (limit of proportionality (LOP), residual)
- NBN B 15-238 : Tests on fibre reinforced concrete - Bending test on prismatic samples

To determine the toughness of the fiber reinforced concrete, usually beam specimens are used. However, many drawbacks have been found in the standard test methods related to the beam tests such as ASTM C 1018 and ASTM C 1399. It has been found that panel test can sort out relative behavior among the various concretes and this test shows inherently low variability. In addition, round panel test is more representative of field performance (Xu, Mindess and Duca 2004).

In this thesis study centrally loaded round and square panels test methods were used as explained below.

### **2.6.1 Centrally Loaded Round Panel Method**

This test method is applied according to the ASTM C1550-12a. The aim of this method is to determine the flexural toughness of the fiber reinforced round panels by using a central load which is applied on the specimen at a specific loading rate. Then, the performance of the specimen is calculated in terms of energy absorption capacity using the central deflections with the corresponding loads. The area under the load and the displacement represents the calculated toughness of the specimen.

In this method, the round panel specimen is placed on the three symmetrically pivots on which the transfer plates are arranged to ensure a smooth and flat platform and the three pivots are arranged with 120 degree angle with respect to each other. At the midpoint of the specimen an LVDT is used to measure the deflection in a precise way with the high sensitivity.

This method well represents the post crack behavior of the fiber reinforced structural members, especially, the mode of failure behavior of the in-situ structures because of the fact that it experiences bi-axial bending in reply to a central point load (ASTM 2012).

According to the ASTM C1550-12a, it has been reported that, the energy absorption capacity which corresponds to a central deflection up to 40 mm, is viable to the situations subjected to severe deformation in situ such as shotcrete in tunnels, temporary support linings in swelling ground etc. Moreover, the corresponding central deflection up to 5 mm can be applicable to obtain the toughness of proposed low levels of deformation exposed areas such as final linings of underground structures.

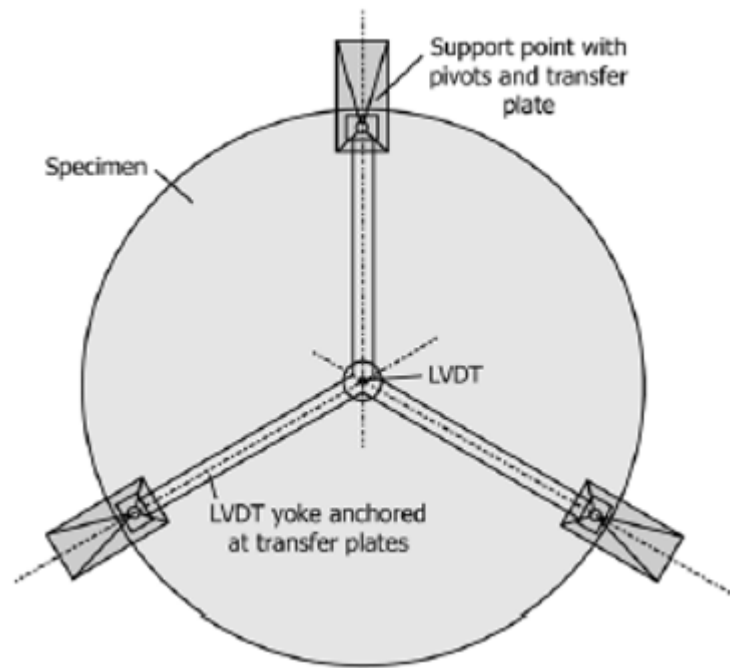


Figure 2.13: Plan view of suggested method of deflection measurement.

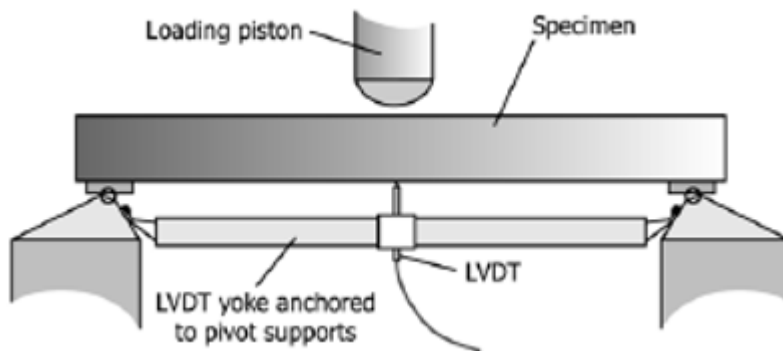


Figure 2.14: Suggested method of deflection measurement to exclude load-train and crushing of concrete at the point of loading using a linear variable deflection transducer (LDVT).

The response measured by the cross head and the LVDT mounted underneath the sample is quite similar. However, at the initial part of the test, the cross head will measure the deformation occurred in the specimen and the test assembly as well. Therefore, the first crack deflection can be measured more accurately through the LVDT (Mobasher 2011).

The three symmetrically 120 degree oriented support pivots lead to low within-batch variability in the energy absorbed by a set of panels up to a specified central deflection.

The most important physical property which strongly affects the panel performance in this test is the thickness of the panels. However, the diameter has a small effect on the result of performance of panel. The nominal dimensions of the panels are 75 mm in thickness and 800 mm in diameters. The displacement rate is about 4.0 mm/min. However, when displacement-controlled testing machine is used, and the surface of the specimen is rough, the effective displacement rate may be less than 4.0 mm/min. As a result of the tests, it has been seen that small changes in the effective rate do not affect the energy absorption value (ASTM 2012). This range can be defined between 0.5 to 10 mm/min.

#### **2.6.1.1 Centrally Loaded Square Panel Method**

Square Panel Test which is also called as “ENFARC Panel Test“ is a toughness measurement test that determine the absorbed energy by load-deformation curve. The test is designated to create more realistically biaxial bending model that may occur in some structural member applications (Rivaz 2015).

Square Panel test is simulating, at a laboratory scale, the structural behavior of the concrete slab under flexural and shear load.

The test setup performed according to the ENFARC Panel test, is presented in Figure 2.15 and Figure 2.16.

The dimensions of the test plate is  $600 \times 600 \times 100 \text{ mm}^3$  and the center point contact



Figure 2.15: ENI14488-5 testing on steel support (Rivaz 2015).

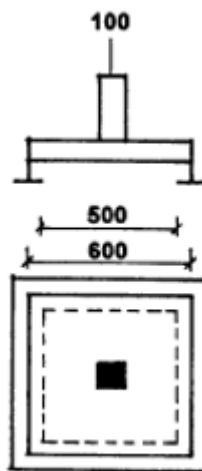


Figure 2.16: Set-up for plate test (EFNARC 1996).

area is  $100 \times 100 \text{ mm}^2$ . The test plate shall be continuously supported on its 4 edges by a steel frame.

The point load is applied at the center of the plate with the help of a rigid smooth block. This block provides a flat surface for the applied load and enables an accurate load distribution. The test is performed at a constant loading rate of 1 mm/min until the deflection reach 30 mm, and the load-deflection data recorded though the whole test (Rivaz 2015).

The square panel test is more convenient than beam test to evaluate the performance of

fiber reinforced concrete, because 4 edges supported specimen simulates the continuity of the in-situ application of concrete lining while, in beam test this continuity cannot be reached. Moreover, the fiber reinforcing effect in a panel is very similar to the real behavior of the slab while in beam test the specimen act along one direction.

#### **2.6.1.2 Comparison and Correlation of Round and Square Plate Test Results**

The square plate is simply supported along the whole perimeter of the specimen therefore; it is an indeterminate structure testing. On the other hand, round panel test is a statically determinate test in which the crack pattern prediction is quite predictable and the post cracking material behavior can be seen easily (Minelli and Plizzari 2010). Moreover, in square plate during the loading phase, some irregular distortions of boundary lines have been observed. The deformed part may go upward and it loses the contact with the support (Han et.al. 2010).

Parmentier et.al (2008), performed an experimental study to compare test results of various test procedures. Four testing methods were used which are Three Point Bending Test according to EN 14651, Four Point Bending Test NBN B15-238, Round Panels according to ASTM C1550-05, Square Panels according to EFNARC. The fiber ratio were  $4.5 \text{ kg/m}^3$  for macro synthetic fiber (0.49% by volume) and  $30 \text{ kg/m}^3$  for the steel fibers (0.38% by volume). The slenderness ratio=50 for steel fibers while for synthetic fibers slenderness ratio were not taken into consideration. In conclusion it was reported that; the variation of the beam test results is higher than of the square and round panel test results. The variation coefficient was reported above 20% in classical beam bending test stated above, however, in round panel and square panel test the variation was reported between 6% and 9%. Therefore, it can be said that in determining the toughness of the materials in different test methods, square and round panel tests give more reliable results compared to the beam test results.

Chao et.al. (2011), made a performance comparison of three different test methods for evaluation of fiber reinforced concrete. The three methods were: i) Third Point Bending Test (ASTM C1609; ASTM, 2007), ii) Uniaxial Direct tensile Test and iii) Round Panel Test (ASTM C1550). It was concluded that:

- In uniaxial direct tensile test, the crack propagation path cannot be controlled well and that led a variation in post cracking response and in the post cracking response, it was seen a significant variability.
  
- In Third Point Bending Test, although the first cracking loads are almost same, the post-cracking response and peak flexural strength shows a considerable variability. This variability may be caused by the non-uniform distribution of fiber along the specimen. Due to this fact, this test methods does not give a consistent result.
  
- In round panel test, it was seen that the change in variation coefficient of peak load and energy absorption versus deflection values were as low as between 5% to 13%. Also, usually the major cracks are produced as a result of this test and this leads to performance is evaluated better freely by the means of fiber distribution. Also, the crack propagation can be seen in round panel test very well. Therefore, as a result of comparison of three test method for fiber reinforced concrete, the round panel test gives more reliable results while evaluating the performance (Chao et.al. 2011).

## CHAPTER 3

### EXPERIMENTAL STUDY

#### 3.1 Experimental Plan

In the scope of this thesis study, fiber reinforced concrete samples prepared with different dosages of polypropylene fibers were tested in accordance with ASTM C155-12 a (Round Panel Test Method) and EFNARC Square Panel Test Method to determine their energy absorption capacity.

The samples were divided into two groups. The first one is “Normal Polypropylene Fiber Dosage Concrete” (NPFC) samples and the other one is “High Polypropylene Fiber Dosage Concrete” (HPFC) samples. In NPFC samples; 3, 6 and 9 kg/m<sup>3</sup> (0.3%, 0.6%, 0.9% by volume respectively) dosages while in HPFC 12, 18 and 24 kg/m<sup>3</sup> (1.32%, 1.67%, 2.64% by volume respectively) dosages polypropylene fibers were used. Moreover, since the use of higher amounts of fibers were not possible, a highly workable matrix was utilized in the mixtures number 2.

For each concrete matrix group, six different samples were prepared. Three of them are for Round Panel Test Method, and the other three are for EFNARC Square Panel Test Method. Therefore, a total of 36 FRC samples were prepared as can be seen in Table 3.1.

Table 3.1: Number of specimens

Label	Concrete Matrix	Fiber Dosage (kg/m <sup>3</sup> )	Round Plate	Square Plate
NPFC 3	#1	3	3	3
NPFC 6		6	3	3
NPFC 9		9	3	3
HPFC 12	#2	12	3	3
HPFC 18		18	3	3
HPFC 24		24	3	3

### 3.2 Mixture Proportions

For the NPFC, 200 kg/m<sup>3</sup> and for the HPFC, 400 kg/m<sup>3</sup> cement was used in the samples. In order to increase the viscosity a higher percentage of fly ash was utilized in the HPFC mixtures. This enabled a homogeneous distribution of higher amounts of fibers. In HPFC samples, there were used higher percentage of fly ash compared to the NPFC samples. Also, superplasticizer amount in HPFC samples were higher than NPFC ones to enable the homogeneous mixture in higher amount of fibers. As a result of the mix proportions, the compressive strengths of the HPFC samples were expected to be higher than NPFC samples.

#### 3.2.1 Cementitious Materials

In this study, CEM-I 42.5 R Ordinary Portland Cement -obtained from Başıtaş Cement Plant, Ankara- was used for all samples. The density of cement was 3.11 g/cm<sup>3</sup> and the blaine fineness was 3700 cm<sup>2</sup>/g. According to the TS-EN 196-3, the initial setting time of cement paste was determined as 185 minutes.

Table 3.2: Mix designs

Label	Concrete Ingredients (kg/m <sup>3</sup> )								
	Cement	SF	FA	W	SP	F	Aggregates		
							Fine	Coarse 1	Coarse 2
NPFC 3	200	0	50	125	3	3	1006	520	520
NPFC 6	200	0	50	125	3	6	1001	518	518
NPFC 9	200	0	50	138	3	9	981	507	507
HPFC 12	400	28	400	232	8	12	757	335	0
HPFC 18	400	28	400	215	8	18	775	344	0
HPFC 24	400	28	400	232	8	24	733	325	0

The major oxide composition of cement is listed below Table 3.3.

Table 3.3: Major oxide composition of cement

Chemical Properties	
Chemical Composition (%)	P.C
SiO <sub>2</sub>	19.15
Al <sub>2</sub> O <sub>3</sub>	5.16
Fe <sub>2</sub> O <sub>3</sub>	3.56
CaO	63.26
MgO	1.28
SO <sub>3</sub>	2.77
Na <sub>2</sub> O	0.30
K <sub>2</sub> O	0.37
P <sub>2</sub> O <sub>5</sub>	-
TiO <sub>2</sub>	-
L.O.I (%)	3.83
Physical Properties	
Density (g/cm <sup>3</sup> )	3.11
Average Particle Size (μm)	-
Surface Area (m <sup>2</sup> /g)	0.37

Moreover, to enhance the workability of the concrete, class F fly ash from Sugözü

thermic power plant was also used in all the mixtures. For HPFC mixtures, silica fume, obtained from Antalya Ferrochrome Plant, was used in order to enhance the strength performance of the concrete.

### 3.2.2 Fiber

The fiber used in this study was, 48 mm length fibrillated Barchip brand Polypropylene fibers (Table 3.1). The mechanical and physical properties of the fibers as specified by the manufacturer are listed in Table 3.4.

Table 3.4: The mechanical and physical properties of fibers (EPC 2016)

<b>Characteristic</b>	<b>Material Property</b>
Base Resin	Modified Olefin
Length	48 mm
Aspect Ratio	52.34
Tensile Strength	640 MPa
Surface Texture	Continuously Embossed
No. Fibers/kg	59500
Specific Gravity	0.91
Young's Modulus	10 GPa
Melting Point	159 -179 °C
Ignition Point	Greater than 450 °C
Appearance	Solid Body
Boiling Point	None - Dissolves
Volatilisation	None
Flammability	Combustible
Oxidation Character	None
Self Reactive	None



Figure 3.1: Polypropylene fiber used

### 3.2.3 Superplasticizer

Since the use of fibers decreases the workability of concrete, a superplasticizer, GLENIUM 51 by BASF company, was used to compensate this loss. The properties of the superplasticizer used in this study as specified by the manufacturer are listed in the following Table 3.5.

Table 3.5: Properties of superplasticizer “Glenium51” from BASF (BASF 2013)

Characteristic	Material Property
Structure of Material	Polycarboxylic ether based
Color	Amber
Density	1.082-1.142 kg/liter
Chlorine Content % (EN 480-10)	< 0.1
Alkaline Content % (EN 480-12)	< 3

### 3.2.4 Aggregates

Three different groups of crushed limestone aggregate were used in this study. The gradations of the aggregates are shown in Figure 3.2. The Standard Test Method for Sieve Analysis of Fine and Coarse Aggregates ASTM C136 was used in gradation.

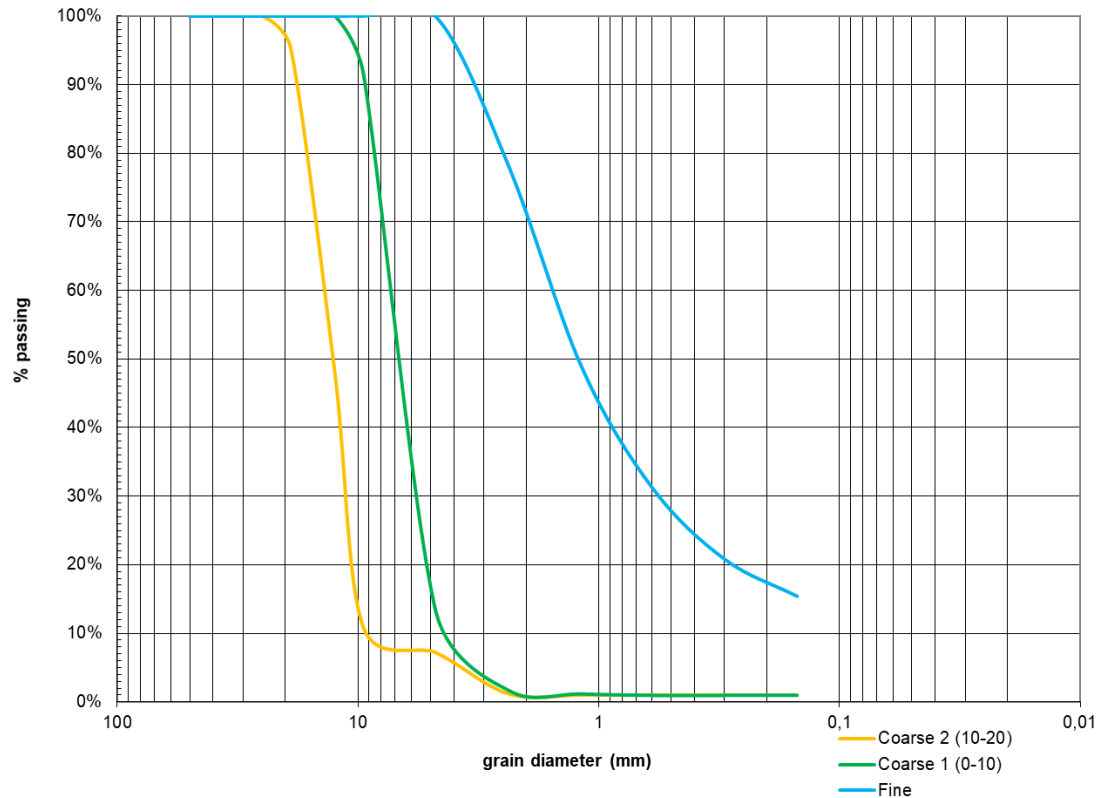


Table 3.6: Aggregate test results

	OD	SSD	ASG	Absorption
Coarse 2	2.64	2.66	2.70	0.86%
Coarse 1	2.67	2.69	2.73	0.83%
Fine	2.58	2.63	2.72	1.94%

OD : Oven-Dry , SSD : Saturated Surface Dry , ASG: Apparent Specific Gravity, Absorption: Water Absorption

### 3.3 Test Equipment

#### 3.3.1 The Molds

For the square panel test, the molds are prepared according to the EFNARC Panel test specifications. The steel molds had dimensions of  $600 \times 600 \times 100 \text{ mm}^3$ .

The round panel molds were also made of steel with a diameter of 600 mm and a thickness of 75 mm. The diameter used for this study was different than the ASTM C-1550 which required 800 mm, because of the limitation on the dimensions of the Loading Frame used in this study.



Figure 3.3: Square and round panel molds W: Width, L: Length, h: Height, D: Diameter.

### **3.3.2 Mixer**

To mix the concrete specimens homogeneously, a rotary electrical mixer with a capacity of 150 L was used.

### **3.3.3 Loading Frame**

The loading frame to test the specimen was an MTS brand universal testing machine with a 250 kN capacity. This machine has a servohydraulic pump that allows to perform precise displacement control tests. The test data were collected by the device itself with a sampling rate of 100 Hz. For each of the round plate and square plate test method, the supports under the plate and the load applying head changes.

For round plate specimens, three points supported base is used and the load is applied through a half spherical head with a diameter of 100 mm. An LVDT was placed at the center of the base to measure the deflection up to 5 mm (the stroke limit of the LVDT used). Through all the test, the displacement control procedure was performed using the values of the axial displacement of the device.

The three points supported base is used when round plate specimen is tested as shown on the Figure 3.5. As mentioned in the previous section, the LVDT is placed at the center of the base to measure the deflection up to a specified limit in more accurate manner. All the test method, is arranged in accordance with ASTM C155-12a with a specimen size of 75 mm in thickness and 600 mm in diameter.

On the other hand, for the square plate specimens a rectangular steel frame was used to make the four edges stand on a simple support. As in the round plates test, the displacement control procedure was performed using the values of the axial displacement of the device. However, no LVDTs were used in this test as it was not required by EFNARC guidance.

Because of the large weight of the specimens, an engine crane was used to place the specimens on the test device.



Figure 3.4: MTS testing machine



a) Round Plate Base

b) Square Plate Base

Figure 3.5: Base plates of the two plate specimens



Figure 3.6: Engine crane

## 3.4 Experimental Procedure

### 3.4.1 The Mixing and Casting Process

At the beginning, the aggregates are placed into the mixer. Then the mixer is turned on for about two to three minutes to allow the aggregates to be mixed homogeneously. Through this period, about 1/5 of the water is added gradually to the aggregate along with half of the fibers to get a better homogeneous mixture and reduce the agglomeration and balling of the fibers. At the end of this period, the cement and the fly ash are added into the mixer and let it run for another two minutes. After this, the rest of the fibers is added to the mixer followed by the rest of the water mixed with the superplasticizer and the silica fume (if the mixture contains silica fume, to allow it to be dispersed in the best way. The mixer is kept running after that for about 5 minutes, and when the materials appear to be fully mixed, the casting process into the molds starts. The samples are kept in the molds for 24 hours before they were removed and stored in continuously wet under ambient room temperature until the test day.

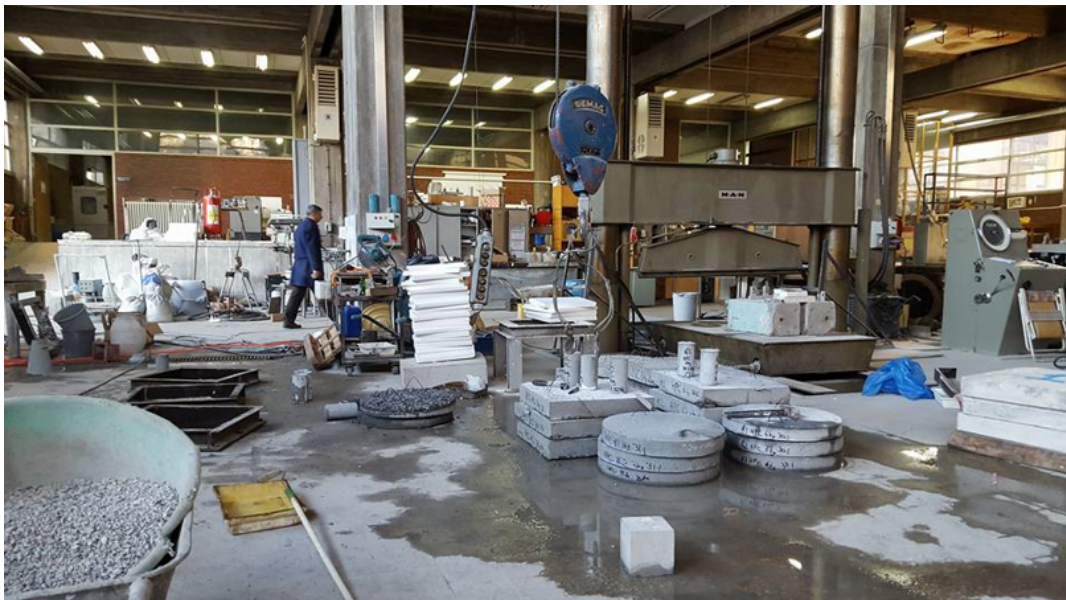


Figure 3.7: A general view of the specimens in the laboratory

### 3.4.2 The Testing Process

After the 28 day curing is completed, the specimens become ready for the test. For the round panel specimens, the LVDT has been placed at the midpoint of three point supported base's bottom part where it measured the deflection of the sample under point load up to 4 mm deflection to get a more accurate result with high precision. After 4 mm deflection is recorded, the LVDT is removed and the device continues to collect the deflection data along with corresponding force values. For square panel test, the procedure is a little bit more complicated compared to round panel test. Because the square panel is supported with a continuous frame, during the test any non-uniformity on the bottom surface and on the edge of the sample may lead to misleading results. Therefore, to avoid that, the steel frame perimeter has been covered with gypsum before the specimen is placed over it. With the help of bubble level, the smooth placement of the sample has been measured. After that, the specimen, along with the frame has been placed on the testing machine for the test.

The deflection limit has been arranged to be up to 30 mm deflection for both square and round panels. However, the evaluation of the data has been performed up to 25 mm deflection in accordance with ASTM C 1550-12a and EFNARC.

Figure 3.8 shows how square and round panel placed on their base on loading frame.



Figure 3.8: The two types of specimen tested a) Square panel b) Round panel

### 3.5 Data Evaluation Method

From the force-deflection graph in Figure 3.9, the energy absorption capacity of each sample has been determined. The area under the force-deflection graph gives the energy absorption capacity or the toughness. As an example, the Figure 3.9 and Figure 3.10 shows the Force-Deflection of Square Panel NPFC 3 sample. The graph represents the measured data collected by the testing device. From the MTS test data, energy absorption capacity is calculated by numerical integration as presented in Figure 3.10.

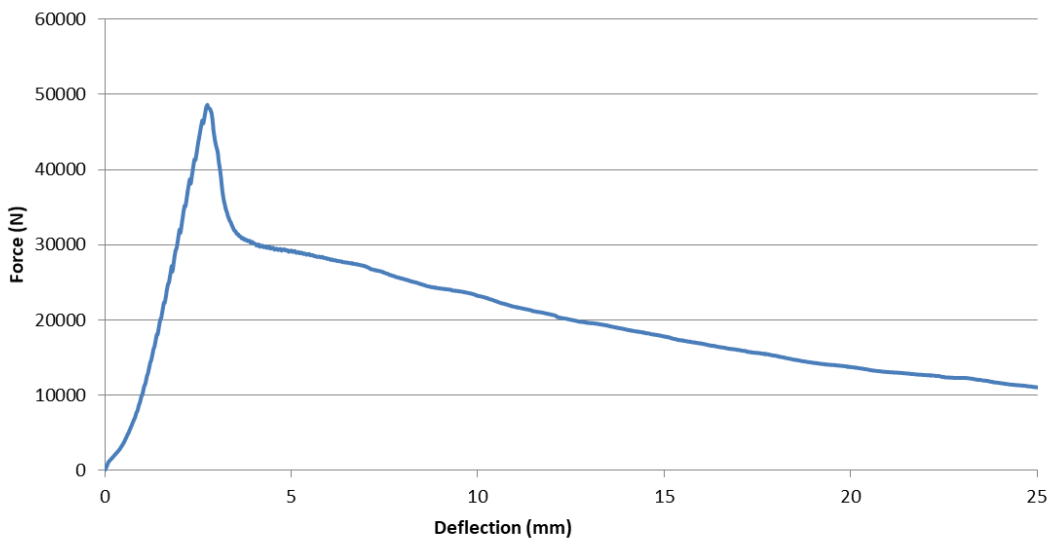


Figure 3.9: Typical force-deflection graph of a square panel

### 3.6 Measuring the Center Point Deflection

LVDTs ensure high sensitivity and precision by measuring the deflection from the bottom of the specimen instead of measuring from the piston. The round panels allow the measurement deflection with the help of LVDT from the bottom. Due to the unavailability of square plate base to place LVDT, the square samples were measured from the piston only. Moreover, in the EFNARC standard there is no statement on the location of center point deflection measurement.

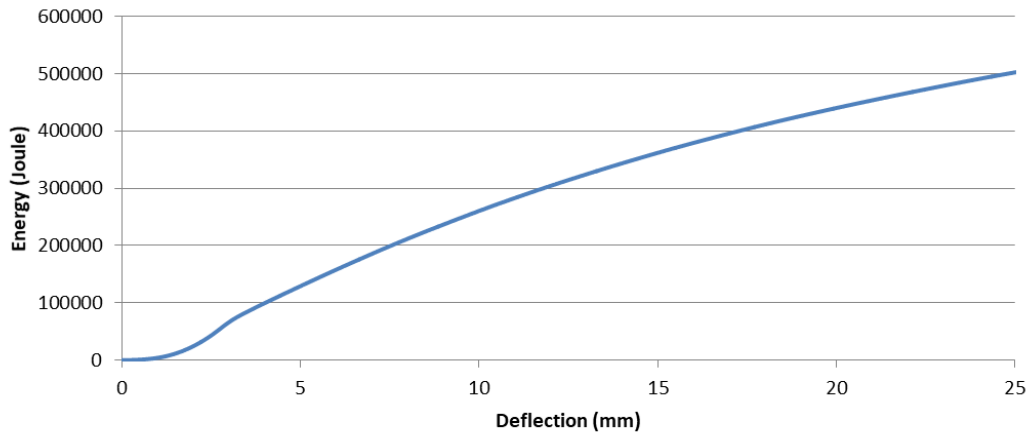


Figure 3.10: Typical energy-deflection graph of a square panel

The Figure 3.11 shows the difference of Force-Deflection graph of the same specimen (HPFDC 18 Round Sample) one of them has LVDT and the other have not. As seen from the two curves the initial slopes of the load-deflection data and the total energy absorption capacity are quite different. However, the energy absorption capacities are almost same. The reason for the change in slope is simply the change in deflection measurement. When the deflections are measured from the piston, the compliance that comes from surface roughness of the concrete and the settlement of the gypsum are all taken into account. Therefore, these deflections are relatively higher when compared to the deflections measured from LVDT.

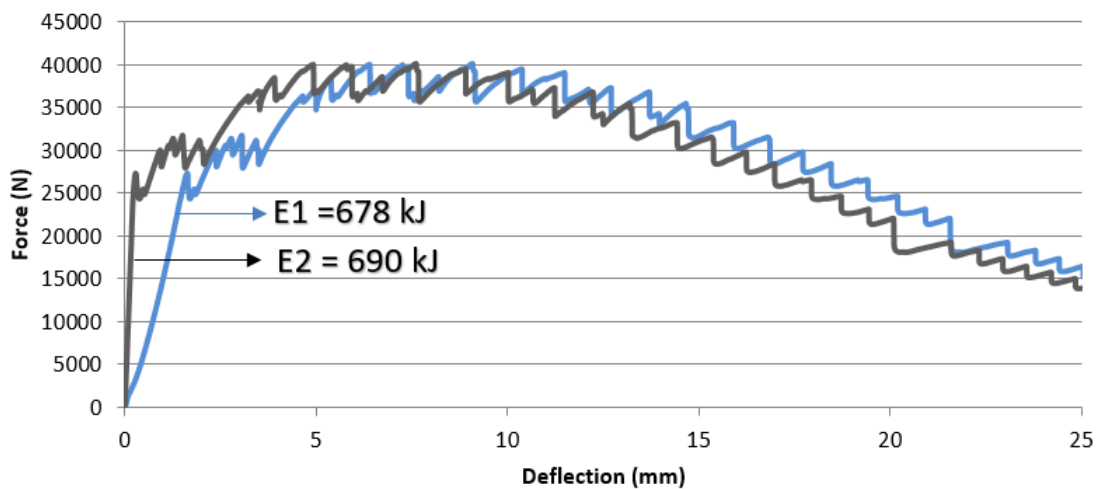


Figure 3.11: Typical force-deflection graph obtained from round plate specimen measured from piston and LVDT

Measuring the deflection from the bottom of the specimen leads avoiding other displacements resulting from the surface irregularity and support conditions.

In this thesis, for the square plate specimens the deflections were recorded from the piston, therefore the compliance that comes with gypsum use all appeared in the load deflection curves, so this should be taken into account.

## CHAPTER 4

### TEST RESULTS

In this thesis study, different dosages of polypropylene fibers have been used and tested in accordance with ASTM C 1550-12a Round Panel Test and EFNARC Square Panel Test methods. The force deflection graphs of the tested specimens are shown in this chapter. Moreover, energy deflection graph of the all tested specimens are given in one chart and the correlation between the round and square panel test data is determined.

#### 4.1 Fresh Concrete Test Results

The table below shows the fresh concrete test data of all six mixtures. Due to the highly viscous nature of HPFC mixes, the slump were measured as slump flow. Unlike this, in NPFC mixes, the zero slump concrete were seen. Typical slump and slump flow figures are seen in Table 4.1.

Table 4.1: Fresh concrete samples test results

Mix Label	Slump/Slump Flow (cm)	Unit Weight (kg/m <sup>3</sup> )
NPFC 3	0	2445
NPFC 6	0	2472
NPFC 9	0	2466
HPFC 12	86*	2217
HPFC 18	74*	2273
HPFC 24	70*	2200
* Slump flow diameter in cm .		



Figure 4.1: a) Slump and b) Slump flow of fresh concrete.

## 4.2 Square Panel Test Data

The square panel test results are shown on the graphs in following subsections.

### 4.2.1 NPFC Square Samples

The force deflection graph and crack patterns of all three mixtures (3, 6 and 9 kg/m<sup>3</sup> fiber dosages) are presented in Figures 4.2, 4.3 and 4.4 respectively. As presented in Figures 4.2, 4.3 and 4.4 each sample has a different thickness. The effect of thickness on the ultimate load or cracking load is quite noticeable. For example, as seen in Figure 4.2, the highest load was obtained from specimen 3 which has the highest thickness among all the three plates. Moreover, the lowest load coincided with the plate having the lowest thickness. This was the case for most of the tested specimens.

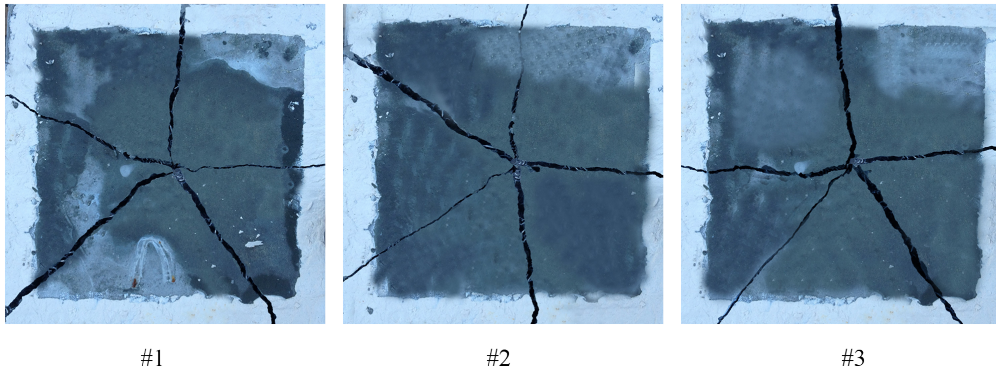
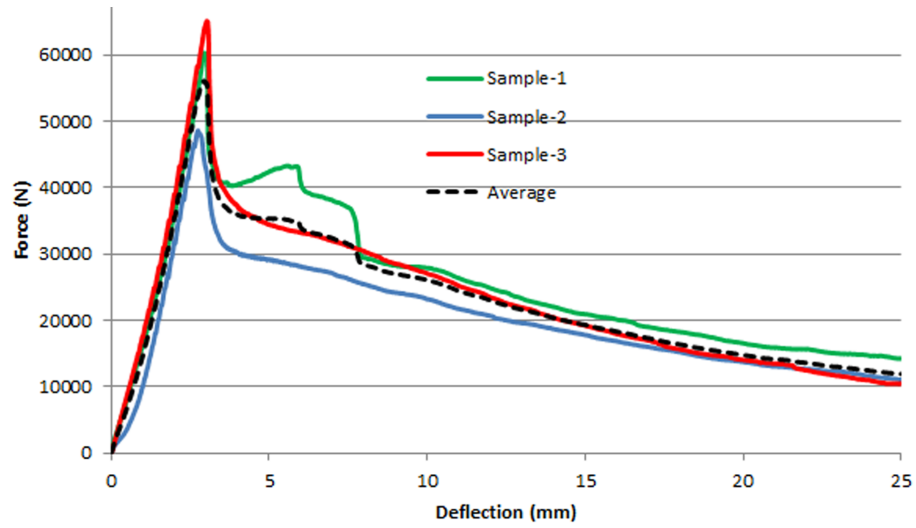


Figure 4.2: Force deflection graph and crack pattern of NPFC 3 square panel samples

Table 4.2: Thickness of NPFC 3 square

Square Panel Thickness		
<i>Label</i>	<i>Sample</i>	<i>Thickness (cm)</i>
<b>NPFC 3</b>	#1	9.69
	#2	9.56
	#3	9.90

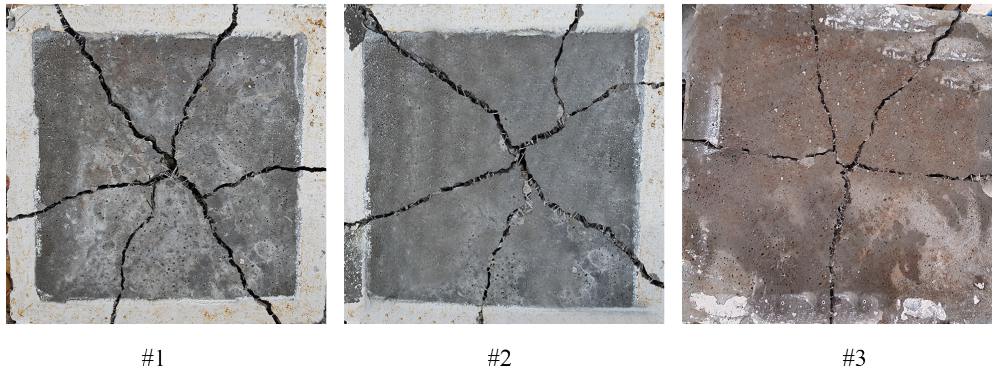
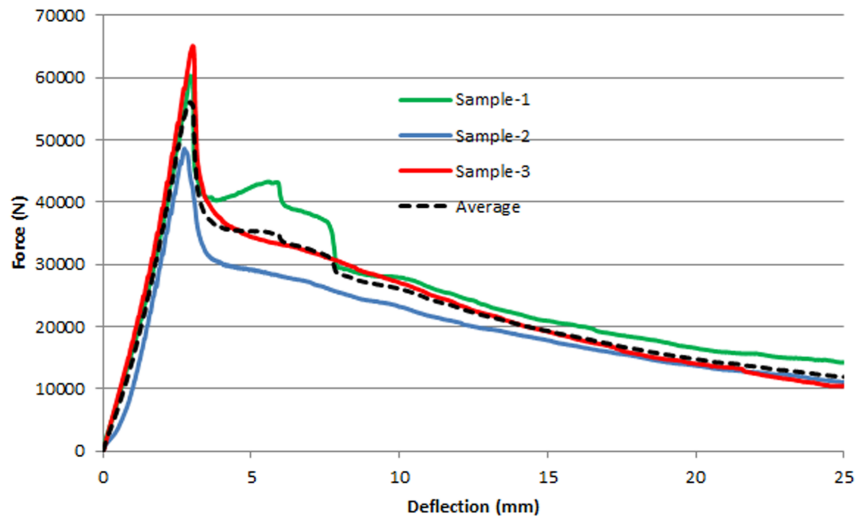


Figure 4.3: Force deflection graph and crack pattern of NPFC 6 square panel samples

Table 4.3: Thickness of NPFC 6 Square

Square Panel Thickness		
<i>Label</i>	<i>Sample</i>	<i>Thickness (cm)</i>
<b>NPFC 6</b>	#1	9.85
	#2	9.66
	#3	10.00

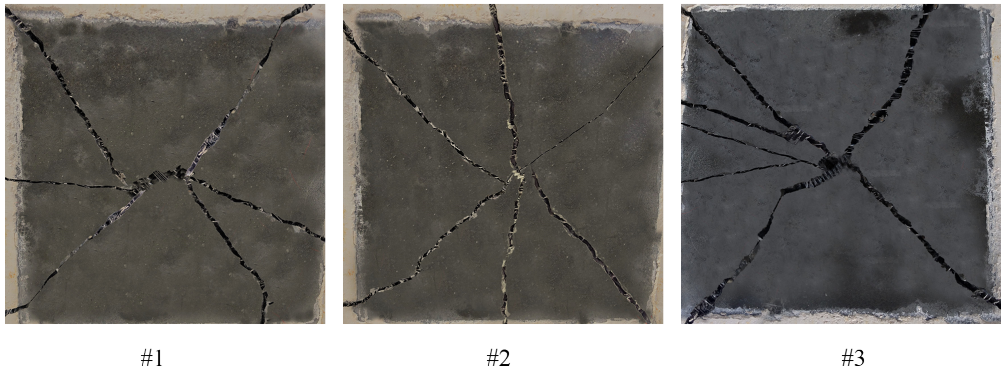
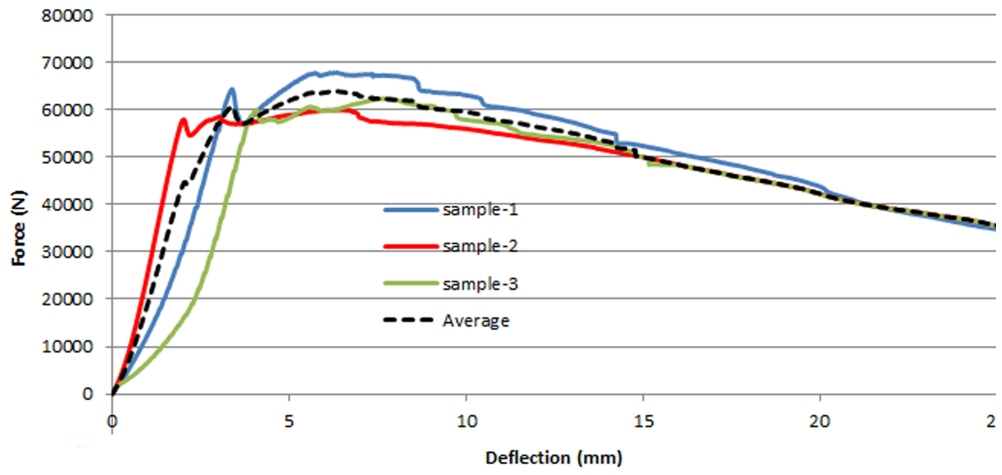


Figure 4.4: Force deflection graph and crack pattern of NPFC 9 square panel samples

Table 4.4: Thickness of NPFC 9 Square

Square Panel Thickness		
<i>Label</i>	<i>Sample</i>	<i>Thickness (cm)</i>
<b>NPFC 9</b>	#1	9.86
	#2	9.63
	#3	9.75

When all the data are combined, the effect of fiber dosage for NPFC 3, 6 and 9 square samples can be seen as presented in Figure 4.5;

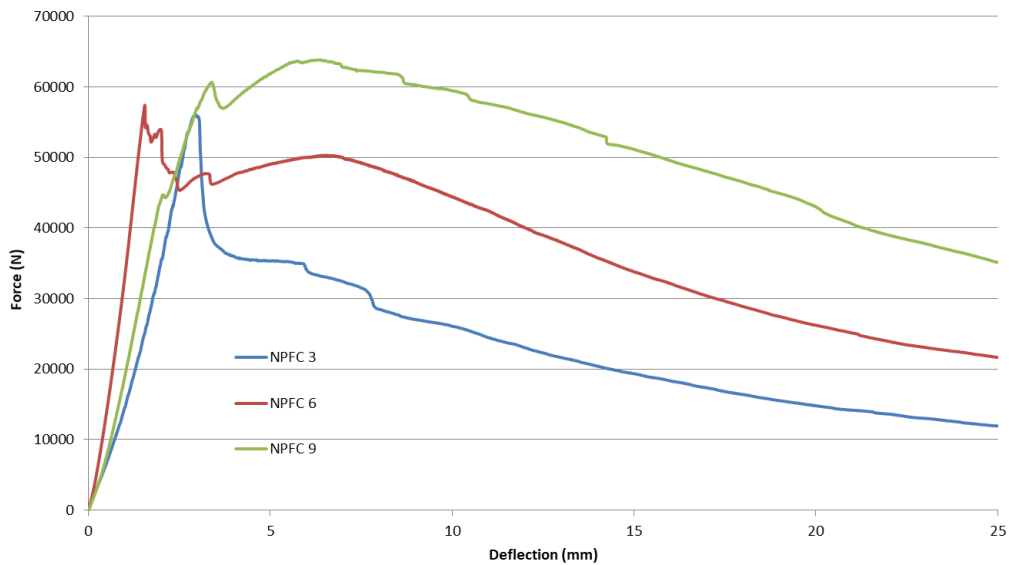


Figure 4.5: Force deflection graph of NPFC 3, 6, 9 square panel samples

As seen in Figure 4.5, with an increase in fiber dosage, there is a considerable improvement in the post-cracking behavior. The post-cracking strength is higher in the NPFC 9 mix. This kind of behavior for low and high volume fraction of fibers were explained by other researchers (Fanella and Naaman 1985) as presented earlier in Figures 2.5 and 2.6.

### 4.2.2 HPFC Square Samples

The force deflection graph and crack patterns of all three mixtures (12, 18 and 24 kg/m<sup>3</sup> fiber dosages) are presented in Figures 4.6, 4.7 and 4.8 respectively.

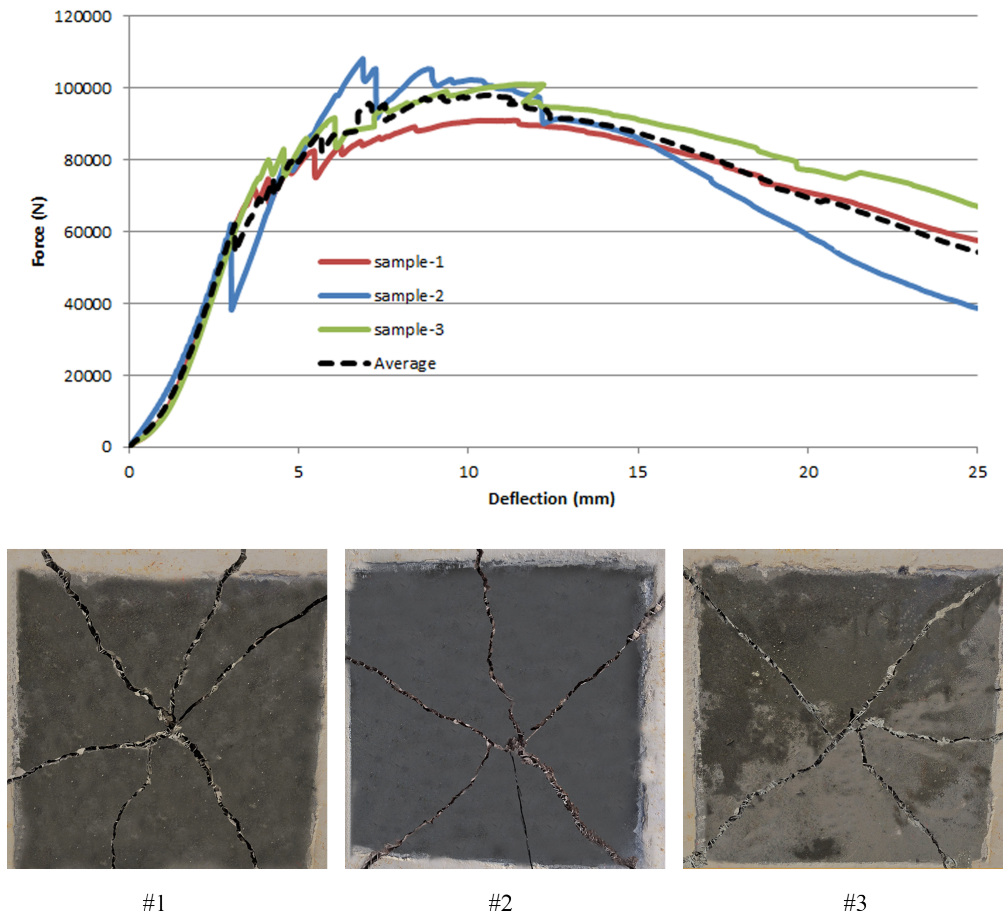


Figure 4.6: Force deflection graph and crack pattern of HPFC 12 square panel samples

Table 4.5: Thickness of HPFC 12 square

Square Panel Thickness		
<i>Label</i>	<i>Sample</i>	<i>Thickness (cm)</i>
<b>HPFC 12</b>	#1	8.86
	#2	9.03
	#3	9.50

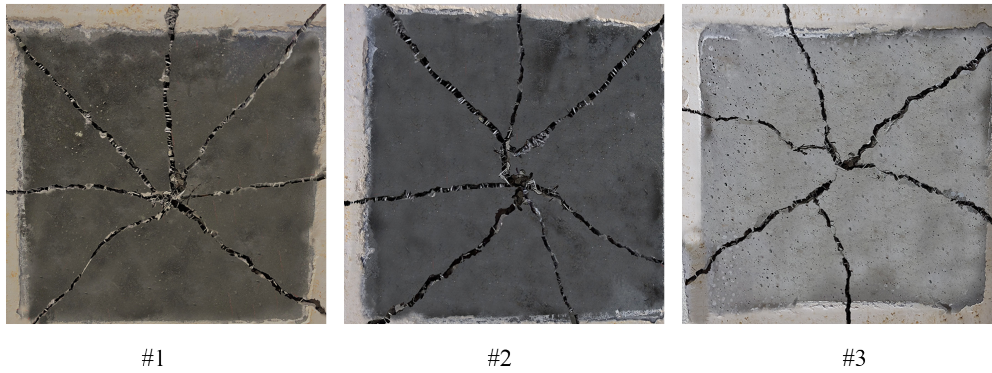
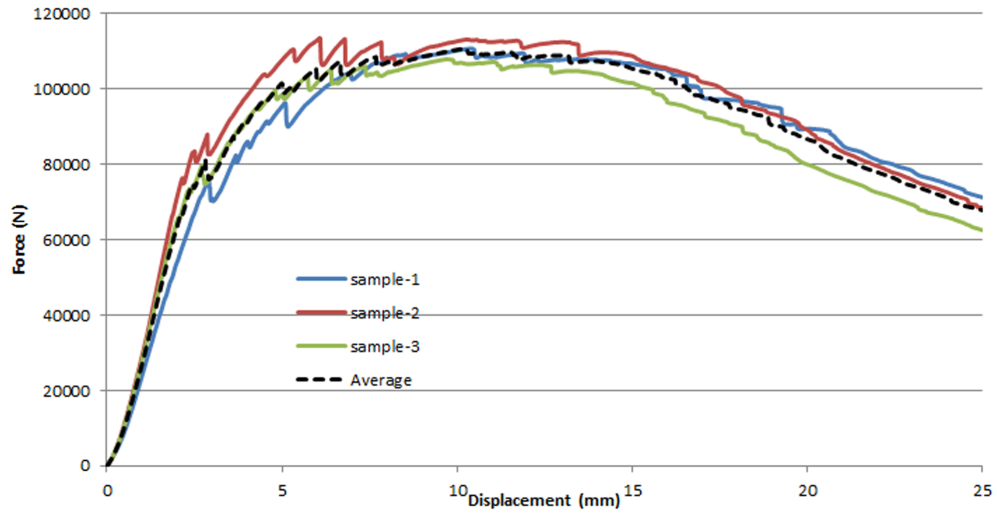


Figure 4.7: Force deflection graph and crack pattern of HPFC 18 square panel samples

Table 4.6: Thickness of HPFC 18 square

Square Panel Thickness		
<i>Label</i>	<i>Sample</i>	<i>Thickness (cm)</i>
<b>HPFC 18</b>	#1	8.90
	#2	9.09
	#3	8.80

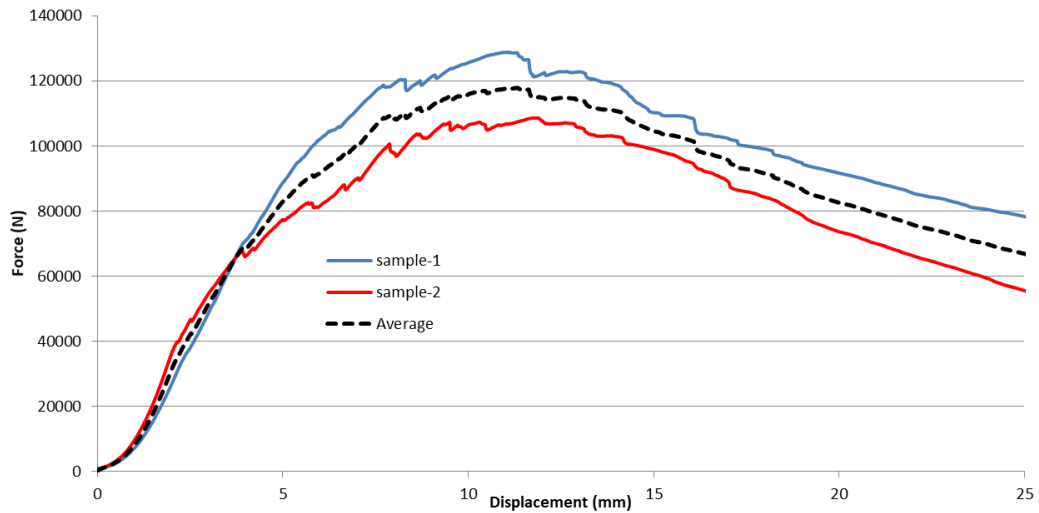


Figure 4.8: Force deflection graph of HPFC 24 square panel samples

The sample-3 data could not be recorded because of an experimental error caused by MTS machine. Also, the crack patterns could not be photographed due to some problems in photographic apparatus.

Table 4.7: Thickness of HPFC 24 square

<b>Square Panel Thickness</b>		
<i>Label</i>	<i>Sample</i>	<i>Thickness (cm)</i>
<b>HPFC 24</b>	#1	8.89
	#2	8.69
	#3	9.00

When all the data are combined, the effect of fiber dosage for HPFC 12, 18 and 24 square samples can be seen as presented in the Figure 4.9;

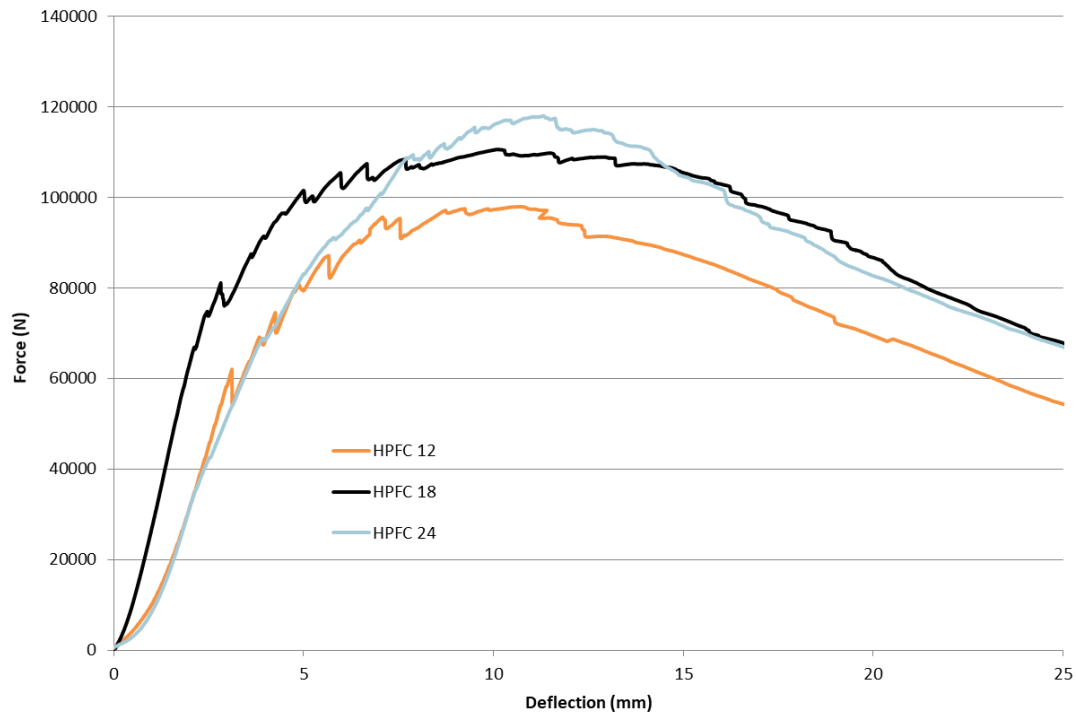


Figure 4.9: Force deflection graph of HPFC 12, 18, 24 square samples

As seen in the Figure 4.9, with an increase in fiber dosage the post cracking strength becomes more obvious and the cracking strength cannot be observed. Moreover, the stiffness of HPFC 18 mixture was quite different than the HPFC 12 and HPFC 24. This was attributed to the measurement of the displacement from the piston. The thickness of the gypsum might have been different when compared to the other two mixtures.

### 4.2.3 Comparison of NPFC and HPFC Square Samples

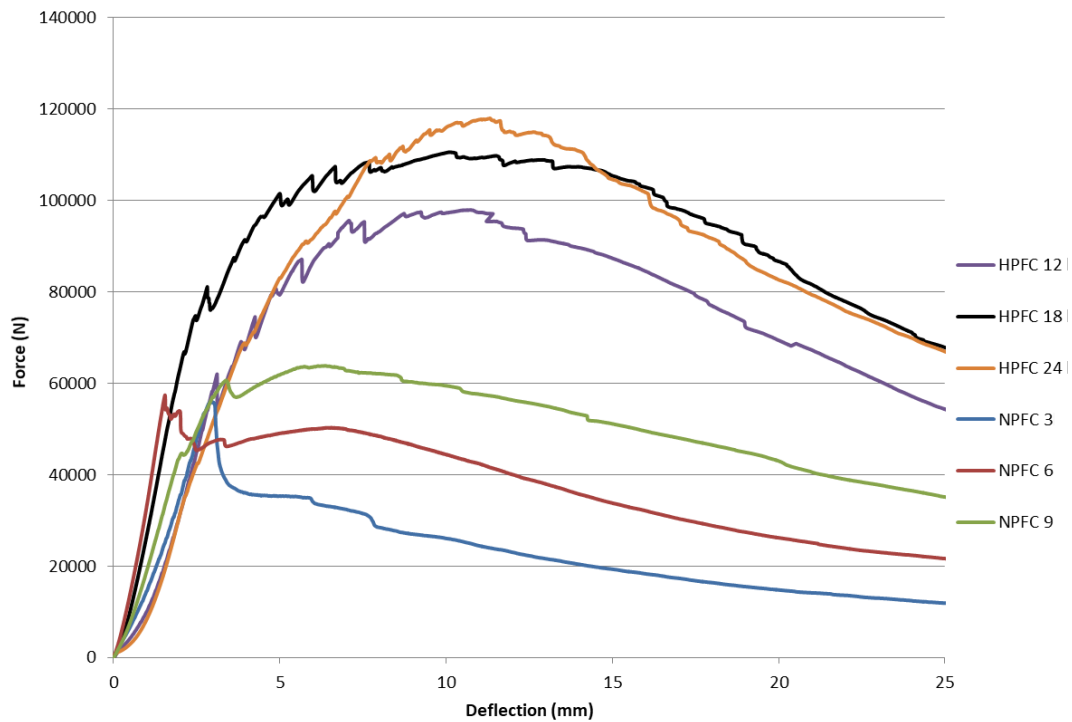


Figure 4.10: Comparison of NPFC and HPFC square samples

To compare the effect of fiber dosage on mechanical performance of FRC mixtures, the average Force-Deflection curves of all mixtures are plotted in Figure 4.10. As seen in that figure, the stiffness (i.e. the slope of Force-Deflection curve in the elastic range ) is quite different for all mixtures and there is no trend. This is simply because of the flaw apparent in the EFNARC test procedure. For correct measurements, the displacement should be measured from the bottom. Nonetheless, the effect of fiber dosage is still visible in that figure. As the amount of fibers increased, the post-cracking behavior is tremendously improved.

The energy-displacement curves are also plotted for comparison.

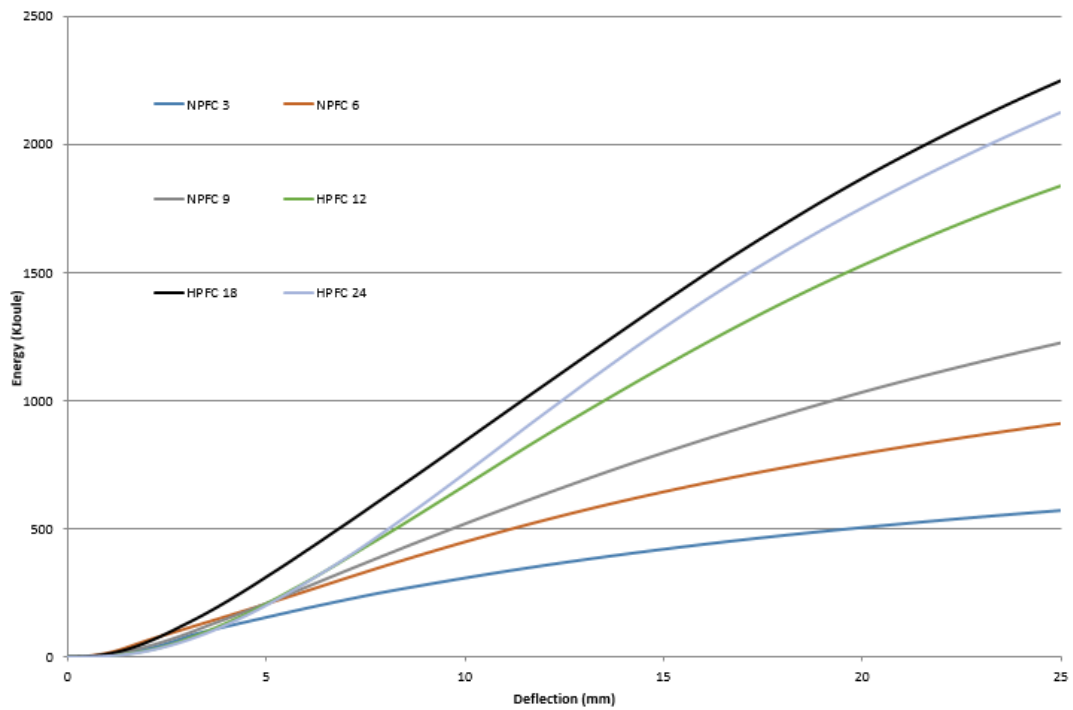


Figure 4.11: Energy deflection comparison of all square panel samples

The amount of energy absorbed is increasing with increasing fiber dosage.

Moreover, the change in energy with the changing volume fraction of fibers is shown in Figure 4.12;

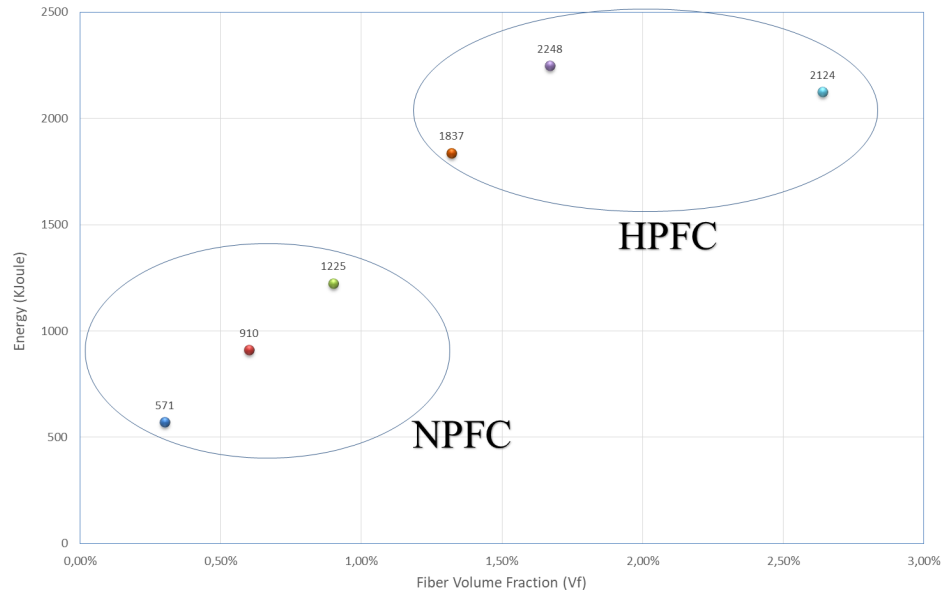


Figure 4.12: Energy vs. fiber volume fraction of square panels

With increasing fiber dosage, energy absorption capacity was increased. However; in HPFC 24, compared to HPFC 18, energy was decreased. This means, for such an amount of fibers in square panel test, the concrete matrix could not meet desired energy increase. The fiber matrix could be changed. For the matrix in use, the optimum fiber dosage was seen as HPFC 18.

### **4.3 Round Panel Test Data**

The round panel test results are shown on the graphs in following subsections.

#### **4.3.1 NPFC Round Samples**

The force deflection graph and crack patterns of all three mixtures (3, 6 and 9 kg/m<sup>3</sup> fiber dosages) are presented in Figures 4.13, 4.14, 4.15 respectively.

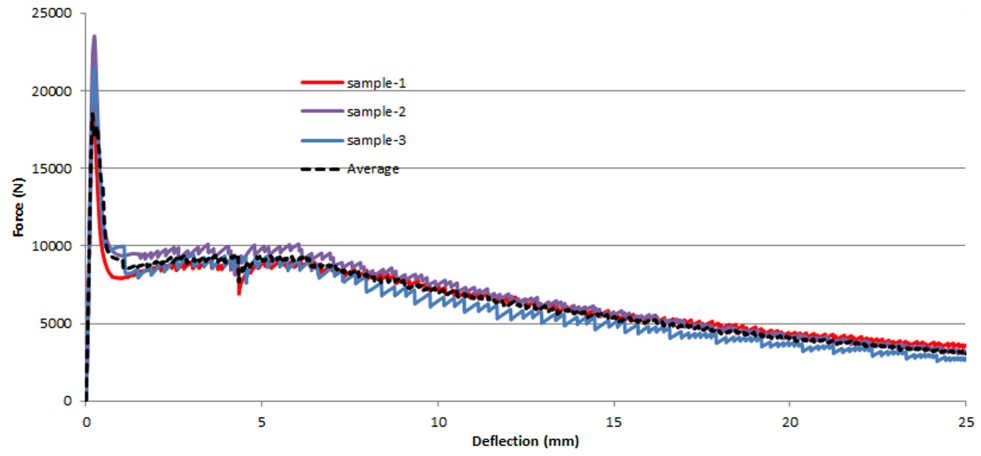


Figure 4.13: Force deflection graph and crack pattern of NPFC 3 round panel samples

Table 4.8: Thickness of NPFC 3 round

<b>Round Panel Thickness</b>		
<i>Label</i>	<i>Sample</i>	<i>Thickness (cm)</i>
<b>NPFC 3</b>	#1	7.11
	#2	7.48
	#3	7.23

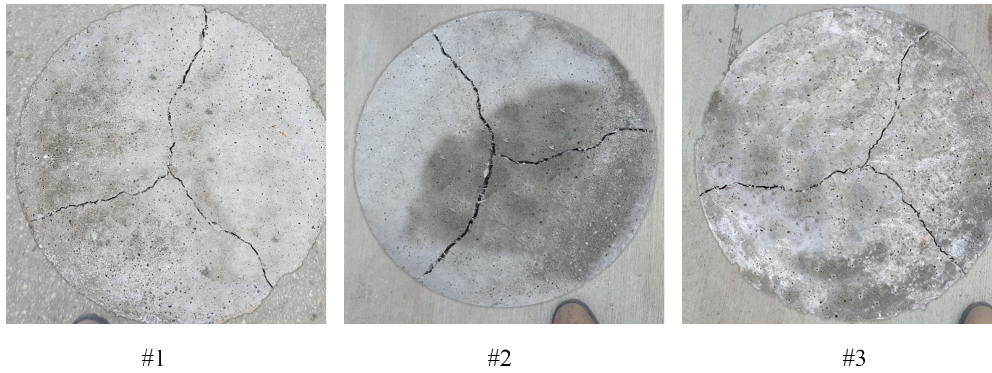
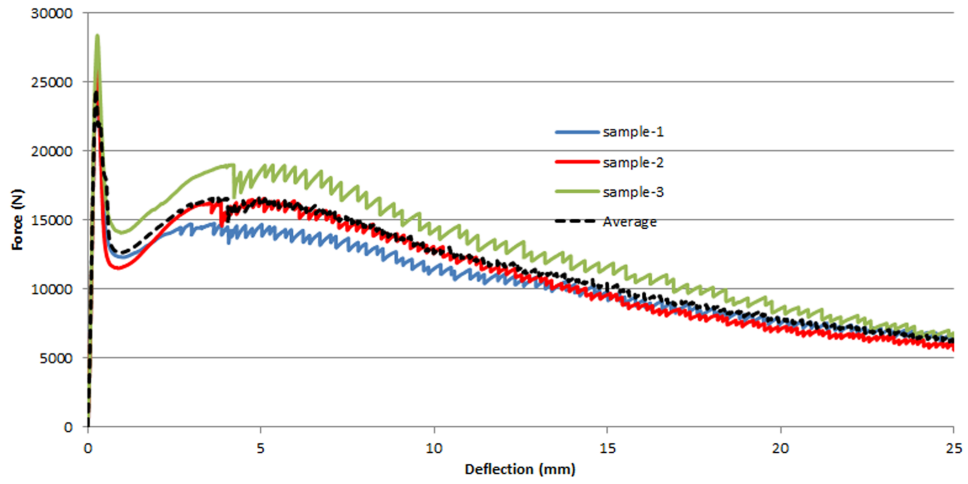


Figure 4.14: Force deflection graph and crack pattern of NPFC 6 round panel samples

Table 4.9: Thickness of NPFC 6 round

<b>Round Panel Thickness</b>		
<i>Label</i>	<i>Sample</i>	<i>Thickness (cm)</i>
<b>NPFC 6</b>	#1	7.10
	#2	7.26
	#3	7.41

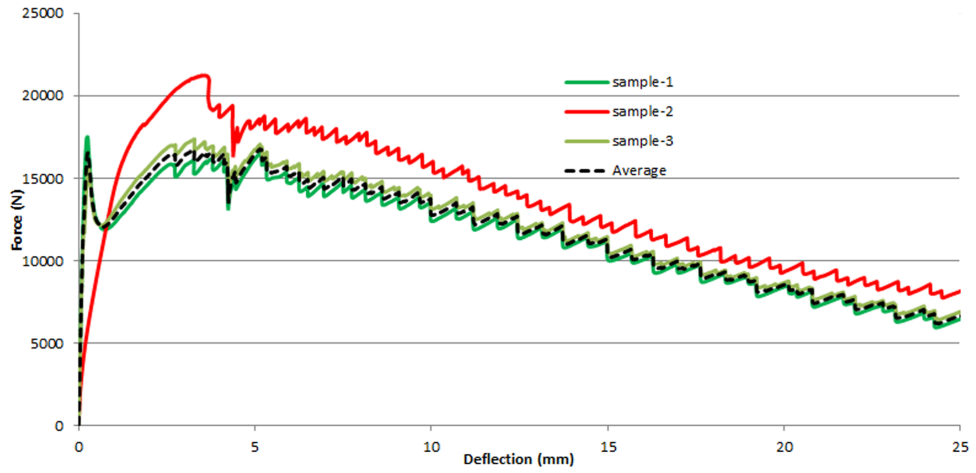


Figure 4.15: Force deflection graph and crack pattern of NPFC 9 round panel samples

Table 4.10: Thickness of NPFC 9 round

<b>Round Panel Thickness</b>		
<i>Label</i>	<i>Sample</i>	<i>Thickness (cm)</i>
<b>NPFC 9</b>	#1	7.28
	#2	7.40
	#3	6.92

For NPFC 9 round, the Force-Deflection graph of sample 2 is different than the others up to first cracking point, this was caused by the slight sliding of the LVDT which leads to misreading. Therefore, it is neglected.

When all the data are combined, the effect of fiber dosage for NPFC 3, 6 and 9 round samples can be seen as presented in the Figure 4.16;

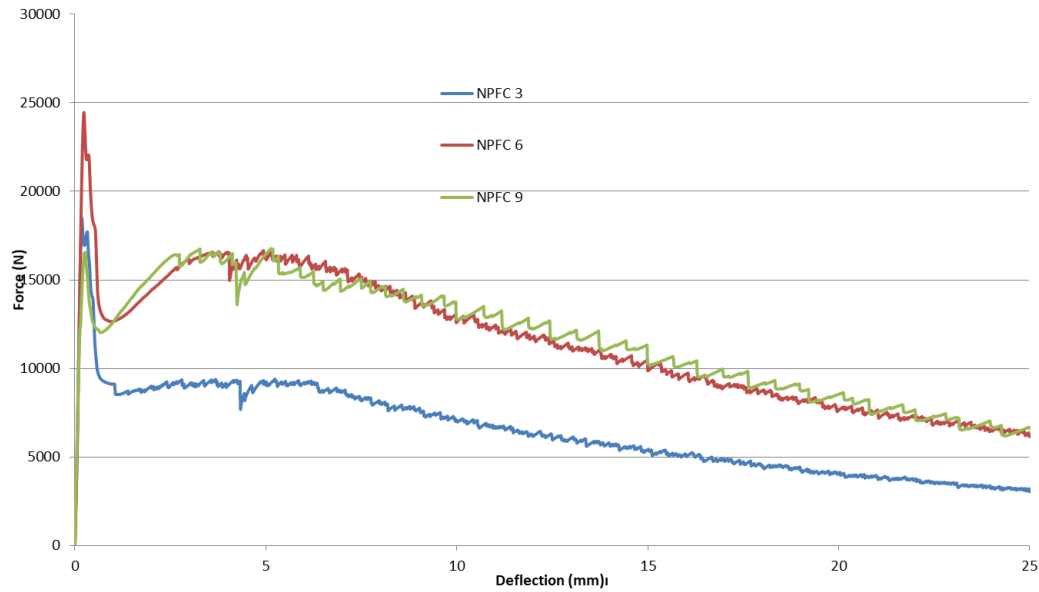


Figure 4.16: Force deflection graph of NPFC 3, 6, 9 round panel samples

As seen in the figure, the cracking load was 18000 N for NPFC 3, 24000 N for NPFC 6 and 15000 N for NPFC 9. This difference is probably due to the variation in the thickness of these specimens. Moreover, it was quite difficult to homogeneously mix NPFC 9 because of the lower viscosity of this mixture. This may have also caused inhomogeneity which may have caused to strength reduction.

### 4.3.2 HPFC Round Samples

The force deflection graph and crack patterns of all three mixtures (12, 18 and 24 kg/m<sup>3</sup> fiber dosages) are presented in Figures 4.17, 4.18 and 4.19 respectively.

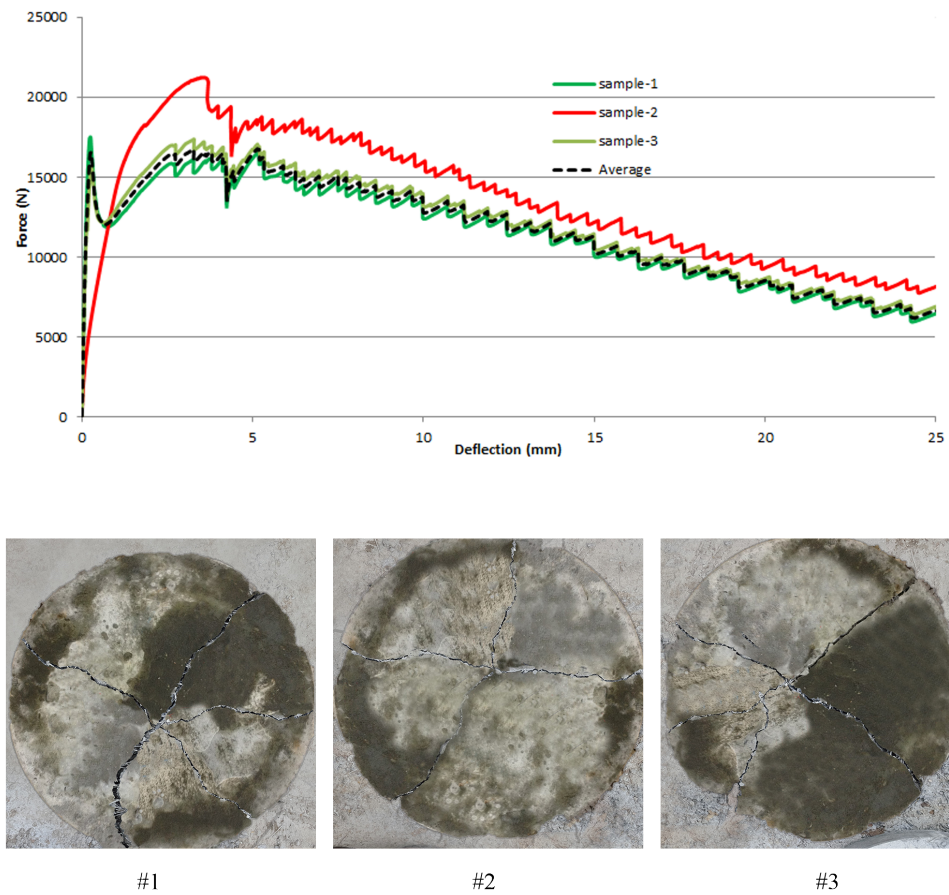


Figure 4.17: Force deflection graph and crack pattern of HPFC 12 round panel samples

Table 4.11: Thickness of HPFC 12 round

Round Panel Thickness		
<i>Label</i>	<i>Sample</i>	<i>Thickness (cm)</i>
<b>HPFC 12</b>	#1	7.49
	#2	7.25
	#3	7.10

The sample-3 data could not be recorded because of an experimental error caused by MTS machine.

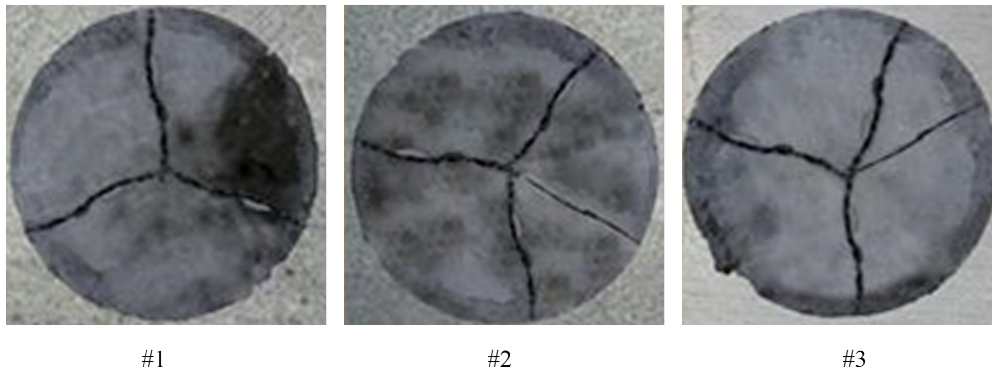
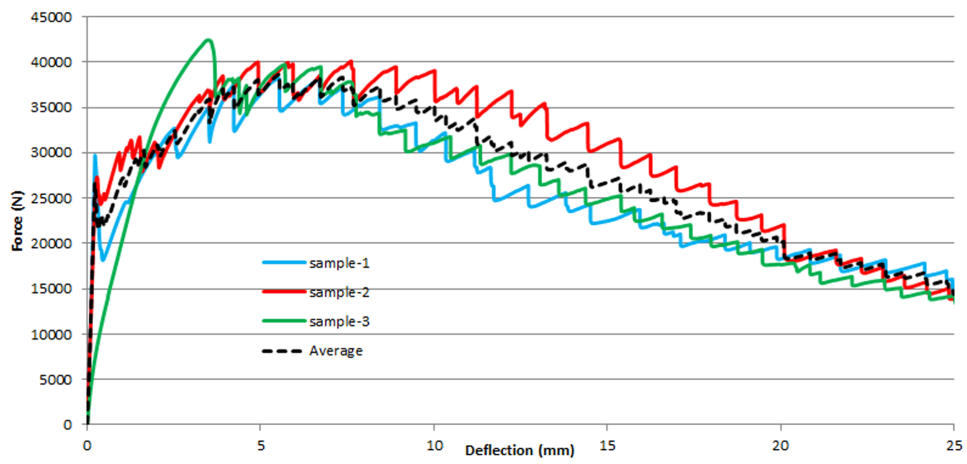


Figure 4.18: Force deflection graph and crack pattern of HPFC 18 round panel samples

Table 4.12: Thickness of HPFC 18 round

Round Panel Thickness		
<i>Label</i>	<i>Sample</i>	<i>Thickness (cm)</i>
<b>HPFC 18</b>	#1	7.25
	#2	7.05
	#3	7.37

For HPFC 18 round, the Force-Deflection graph of sample 3 is different than the others up to first cracking point, this was caused by the slight sliding of the LVDT which leads to misreading. Therefore, it is neglected.

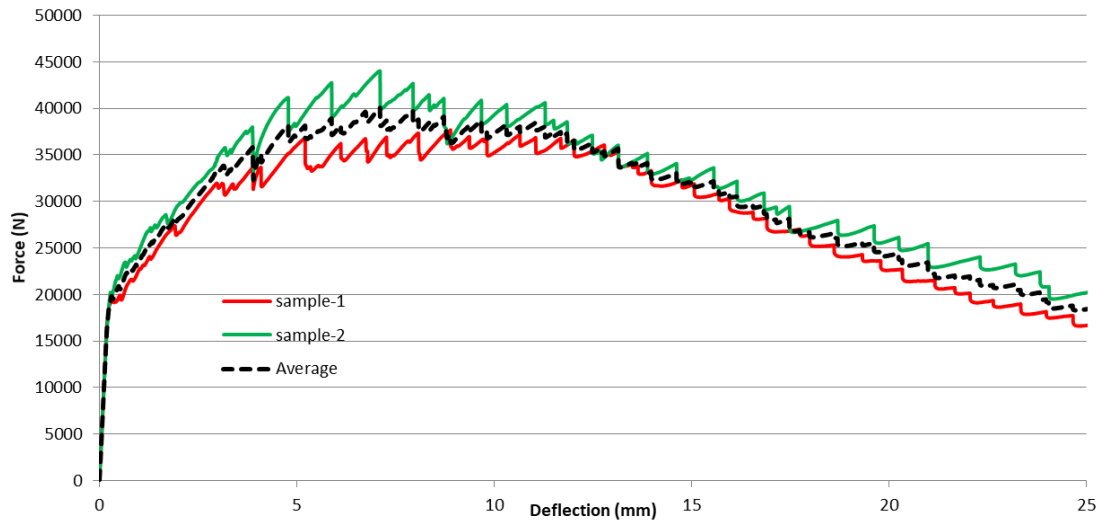


Figure 4.19: Force deflection graph of HPFC 24 round panel sample

The sample-3 data records could not be read because of an experimental error caused by MTS machine.

Table 4.13: Thickness of HPFC 24 round

<b>Round Panel Thickness</b>		
<i>Label</i>	<i>Sample</i>	<i>Thickness (cm)</i>
<b>HPFC 24</b>	#1	7.49
	#2	7.20
	#3	7.35

When all the data are combined, the effect of fiber dosage for HPFC 12, 18 and 24 round samples can be seen as presented in Figure 4.20;

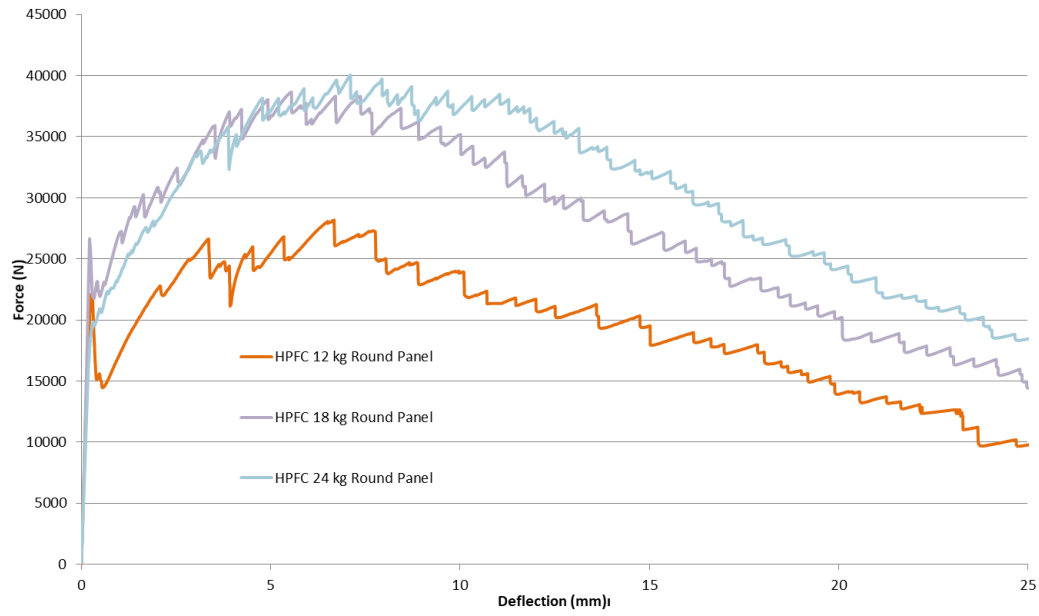


Figure 4.20: Force deflection graph of HPFC 12, 18, 24 round panel samples

### 4.3.3 Comparison of NPFC and HPFC Round Samples

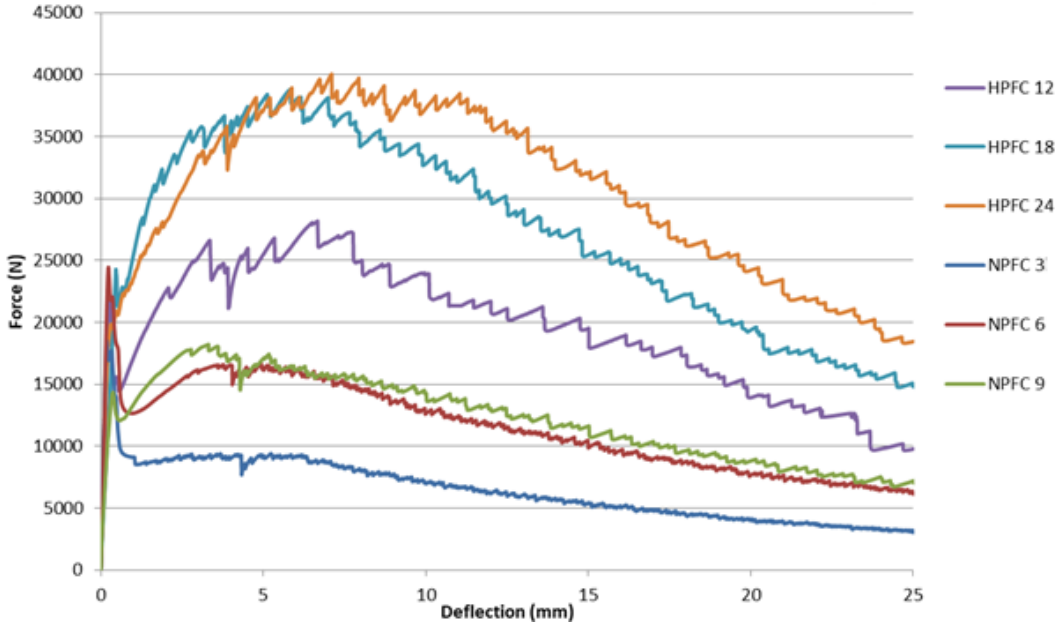


Figure 4.21: Comparison of NPFC and HPFC round samples

When all 6 mixtures are compared in Figure 4.21, the strain hardening behaviour observed in HPFC mixtures are more clear.

The energy vs. displacement curve are also plotted for comparison.

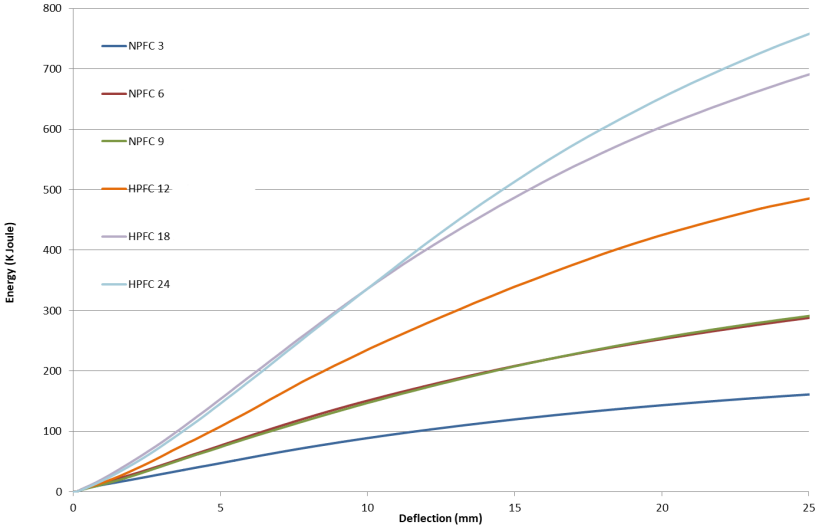


Figure 4.22: The Energy vs. deflection comparison of all round panel samples.

The change in energy with the changing volume fraction of fibers is shown in Figure 4.23;

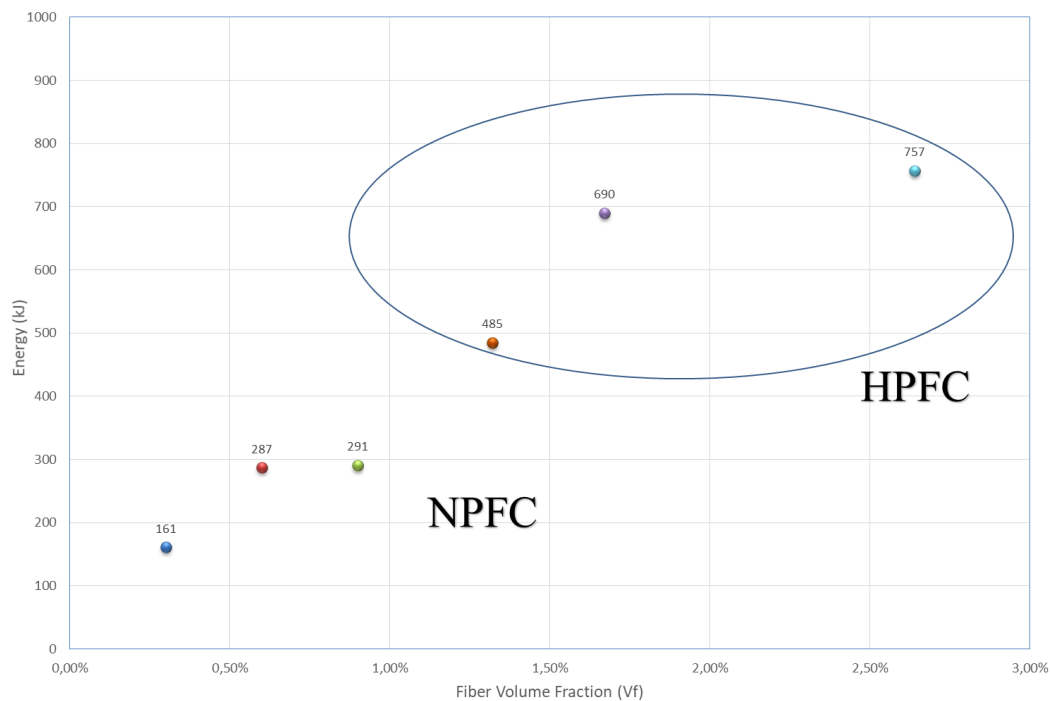


Figure 4.23: Energy vs. fiber volume fraction of round panels

With increasing fiber dosage, energy absorption capacity was increased. However; in HPFC 24, compared to HPFC 18, energy was slightly increased. This means, for such an amount of fibers in round panel test, the concrete matrix could meet the energy increase but not to the desirable amounts. The fiber matrix could be changed to get the maximum capacity of HPFC 24 . For the matrix in use, the optimum fiber dosage was seen as HPFC 18 as in the case square panel test results.

#### 4.4 Round vs Square Plate Energy Relationship

In accordance with the test data, when the maximum energy of the samples which are reached is obtained, the energy relationship between round panel and the square panel samples are compared and a relationship have been found as shown below in Figure 4.24.

Table 4.14: Maximum energy in different volume fractions for round and square panels

	<i>NPFC</i>	<i>NPFC</i>	<i>NPFC</i>	<i>HPFC</i>	<i>HPFC</i>	<i>HPFC</i>
Fiber Dosage (kg/m <sup>3</sup> )	3	6	9	12	18	24
Volume Fraction (Vf)	0.3%	0.6%	0.9%	1.32%	1.67%	2.64%
Round Panel Max. Energy (kJ)	174	309	315	495	733	814
Square Panel Max. Energy (kJ)	626	1010	1387	2108	2518	2430

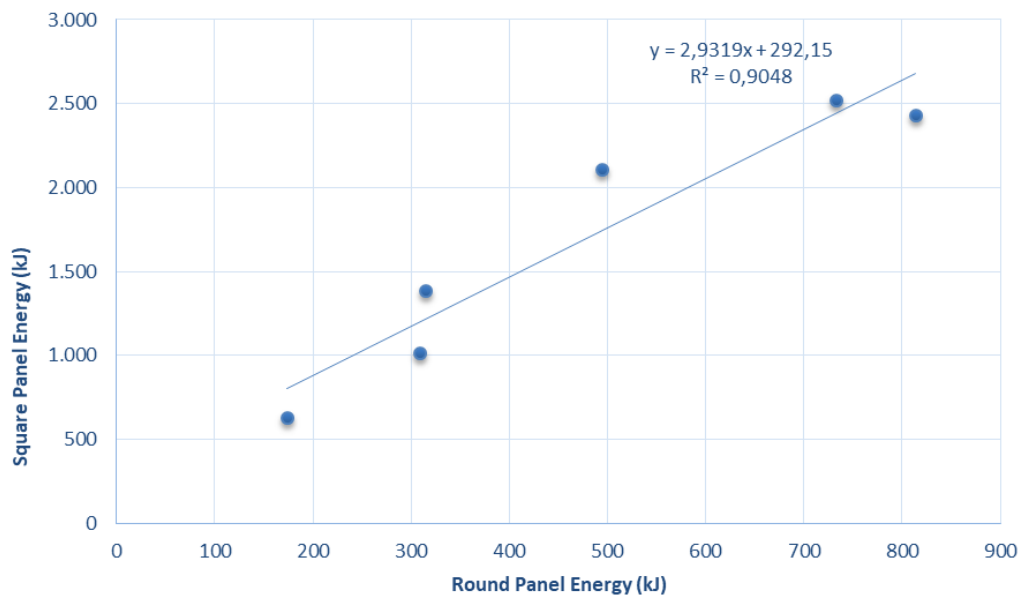


Figure 4.24: Relationship of energy obtained from square and round panel tests



## CHAPTER 5

### CONCLUSION AND RECOMMENDATION

#### 5.1 Conclusion

In this study, high dosage polypropylene FRC (12, 18 and 24 kg/m<sup>3</sup>) and normal dosage polypropylene FRC (3, 6 and 9 kg/m<sup>3</sup>) with different matrix formulations (low viscosity and high viscosity mixtures) were prepared and tested by two different test methods. As a result of this experimental program the following conclusions can be drawn:

- In square panel test, the deflection under the load were measured from the piston, on the contrary, in round panel test it was measured by LVDT. In piston measurement, to avoid the non-uniformity of the specimen surface which were in contact with loading piston, the smooth gypsum layer was created on the contact surface. Therefore, it was hard and time-consuming to specify the gypsum thickness at a specific desired thickness. The gypsum thickness played a role at the displacement was measuring from the piston. However, in LVDT, because the deflection were measured from the bottom of the specimen, there were no such a problem. Therefore, the gypsum factor was eliminated while using round panel test.
- To force all fibers use at its maximum capacity, a strong matrix is needed. In order to achieve optimum efficiency of fiber, the matrix strength should be as high as fiber strength. In thesis study, it was seen that at the matrix in which 24 kg/m<sup>3</sup> fiber dosage in both square and round panel test methods, the energy increase could not reach to desirable levels even a reduction was seen in round panel test method. To reach the desirable levels of energy increase at 24 kg/m<sup>3</sup>

fiber dosage, the concrete matrix should be changed. A stronger matrix can meet the greater amount of fiber dosages.

- For the same concrete matrix and in same fiber dosage, the difference in flexural strength can be explained by thickness of the specimens. The slab thicknesses verify these phenomena as in the seen force-deflection graphs. The thicker samples resulted in greater flexural strength.
- Crack patterns were predictable in round panel test method because of determinate support conditions, but in square panel test methods crack patterns were not predictable. It was seen that the greater energy absorption capacity resulted in increase in total crack lengths especially in square panel test method.
- Friction is the one of the most distinguished property between the two test methods. In square panel test, the rectangular base was used and this rectangular base embrace the sample along the whole perimeter. Likewise as in the top of the specimen on which the load was applied, to ensure the smooth surface between the base and specimen, the gypsum was also used again between the base and specimen. Hence, when the load was applied, during the deformation a friction was created by means of rubbing and dragging. However, in round panel samples, at 120 degree placed pin supported base was used and while the sample begins to deformation, the friction between the support hinges and specimen was as low as considered its effect negligible. Therefore, it can be said that round panel is a friction-free operation unlike as it was in square.
- Round Panel Test is a determinate test method. Square Panel Test is an indeterminate test. Round Panel Test, because of the its statically determinate property, represents better biaxial flexural capacity of FRC. Because, the round panel test and square panels test are different in statically determinacy perspective, the energy measured from the two tests are different than each other.

## **5.2 Recommendation**

It was observed that for further studies, the displacement in the EFNARC test should be measured from the bottom in order to eliminate the intrusion of gypsum in the test results. Moreover, analytical studies can also be conducted in order to eliminate the thickness and geometry effects.



## REFERENCES

- Abbas, Y. M., & Khan, M. I. (2016). Fiber–Matrix Interactions in Fiber-Reinforced Concrete: A Review. *Arabian Journal for Science and Engineering*, 41(4), 1183-1198.
- ACI (2012). State of the Art Report on Fiber Reinforced Concrete Reported. *ACI Structural Journal* 96,(544), 66.
- Akkaya, Y., Shah, S. P., & Ankenman, B. (2001). Effect of Fiber Dispersion on Multiple Cracking of Cement Composites. *Journal of Engineering Mechanics*, 127(4), 311-316.
- Anbuvelan, K. (2014). Strength And Behavior Of Polypropylene Fibre In Impact Characteristics Of Concrete. *American Journal of Engineering Research (AJER)*, 3(8), 55-62.
- ASTM (2012). Standard Test Method for Flexural Performance of Fiber-Reinforced Concrete (Using Beam With Third-Point Loading). *ASTM International, C1550 - 12a*
- ASTM (2012). Standard Test Method for Flexural Performance of Fiber-Reinforced Concrete (Using Beam With Third-Point Loading). *ASTM International, C1609 / C1609M - 12*.
- Bentur, A., & Mindess, S. (2007). *Fibre Reinforced Cementitious Composites*. London: Taylor & Francis.
- Bothma, J. (Eds.) (2015). *Literature Review on Macro Synthetic Fibres in Concrete*. Institute of Structural Engineering, University of Stellenbosch.
- Ceylan, S. (2014). Comparative Evaluation of Steel Mesh, Steel Fiber and High Performance Polypropylene Fiber-Reinforced Concrete in Panel/Beam Tests. *M.S. Thesis*, Middle East Technical University.

- Daniel, J. I., & Gopalaratnam, V. S. (Eds.). (2002). State-of-the-Art Report on Fiber Reinforced Concrete. *ACI Journal Proceedings*, 70(11).
- EFNARC (1993). *European Specification for Sprayed Concrete Report*. Experts for Specialized Construction and Concrete Systems
- Ezeldin, A. S., & Lowe, S. R. (1991). Mechanical Properties of Steel Fiber Reinforced Rapid-Set Materials. *ACI Materials Journal*, 88(4), 384-389.
- Fanella, D. A., & Naaman, A. (1985). Stress-Strain Properties of Fiber Reinforced Mortar in Compression. *ACI Journal Proceedings*, 82(4), 475-483.
- FHA (2005). *Silica Fume User Manual*. US Department of Transportation.
- Hameed, R., et.al. (2009). Metallic Fiber Reinforced Concrete: Effect Of Fiber Aspect Ratio On The Flexural Properties. *ARPN Journal of Engineering and Applied Sciences*, 4(5).
- Jain, D. & Kothari, A. (2012). Hair Fibre Reinforced Concrete. *Research Journal of Recent Sciences*, 1(ISC-2011), 128-133.
- Kalpakjian, S., & Schmid, S. R. (2014). *Manufacturing Engineering and Technology*. Singapore: Pearson.
- Kumar, T. N. (2015). An Experimental Study on Mechanical Properties of Human Hair Fibre Reinforced Concrete (M-40 Grade). *IOSR Journal of Mechanical and Civil Engineering*, 12(4), 65-75.
- Mao, L., & Barnett, S. (2017). Investigation of Toughness of ultra High Performance Fibre Reinforced Concrete (UHPFRC) Beam Under Impact Loading. *International Journal of Impact Engineering*, 99, 26-38.
- Mobasher, B. (2011). *Mechanics of Fiber and Textile Reinforced Cement Composites*. CRC Press.
- Moghimi, G. (2014). Behavior of Steel-Polypropylene Hybrid Fiber Reinforced Concrete. *M.S. Thesis*, Eastern Mediterranean University.
- Mohamed, R. A. S. (2006). Effect Of Polypropylene Fibers On The Mechanical Properties Of Normal Concrete. *Journal of Engineering Sciences, Assiut University*, 34(4), 1049-1059.

- Mohod, V. M. (2015). Performance of Polypropylene Fibre Reinforced Concrete. *IOSR Journal of Mechanical and Civil Engineering*, 12(1), 28-36.
- Parmentier, B. & Vandewalle, L. & Rickstal, F. V. (2008). Evaluation Of The Scatter Of The Postpeak Behaviour Of Fibre Reinforced Concrete In Bending: A Step Towards Reliability. *7th RILEM Symposium on Fibre Reinforced Concrete BEFIB2008 1*, 133–143.
- Ramujee, K. (2013). Strength Properties Of Polypropylene Fiber Reinforced Concrete. *International Journal of Innovative Research in Science, Engineering and Technology*, 2(8).
- Rivaz, B. (2015). Fibre Reinforced Spray Concrete: Minimum Performance Requirement To Meet Safety Needs. *Engineering Conferences International*.
- Robins, P. J., Austin, S. A., & Peaston, C. H. (1989). Toughness Testing of Fibre Reinforced Concrete. *Composite Structures* 5, 729-742.
- Scanfibre, C. P. (n.d.). Flexural Toughness Testing. *Concrete P*, 5–6.
- Shah, S. P., & Daniel, J. I. (Eds.). (1999). Measurement of Properties of Fiber Reinforced Concrete. *ACI Materials Journal*, 85(6).
- Shah, S. P., Daniel, J. I., Ahmad, S. H., Arockiasamy, M., Balaguru, P. N., Ball, C. G., Guerra, A. J. (1988). Measurement of Properties of Fiber Reinforced Concrete. *ACI Materials Journal*, 85(6), 583-593.
- Singh, S. K. (2011). Polypropylene Fiber Reinforced Concrete: An Overview. Retrieved January 22, 2018, from [www.nbmcw.com/concrete/26929-pfr.html](http://www.nbmcw.com/concrete/26929-pfr.html)
- Suksawang, N. & Mirmiran, A. (2014). *Use of Fiber Reinforced Concrete for Concrete Pavement Slab Replacement*. Research Center Florida Department of Transportation .
- Tavakoli, M. (1994). Tensile And Compressive Strengths Of Polypropylene Fiber Reinforced Concrete. *ACI Special Publications*, 142(4).
- UDT (1994). High Performance Concrete, a State of Art Report. *Federal Highway Administration Research and Technology*, FHWA-RD-97-030, 128–133.

- Vallittu, P. K. (2015). High-aspect Ratio Fillers: Fiber-reinforced Composites And Their Anisotropic Properties. *Dental Materials*, 31(1), 1-7.
- Wafa, F. (1990). Properties & Applications of Fiber Reinforced Concrete. *Journal of King Abdulaziz University-Engineering Sciences*, 2(1), 49-63.
- Xu, H., Mindess, S., & Duca, I. J. (2004). Performance Of Plain And Fiber Reinforced Concrete Panels Subjected To Low Velocity Impact Loading. *6th RILEM Symposium on Fibre-Reinforced Concretes (FRC)*.